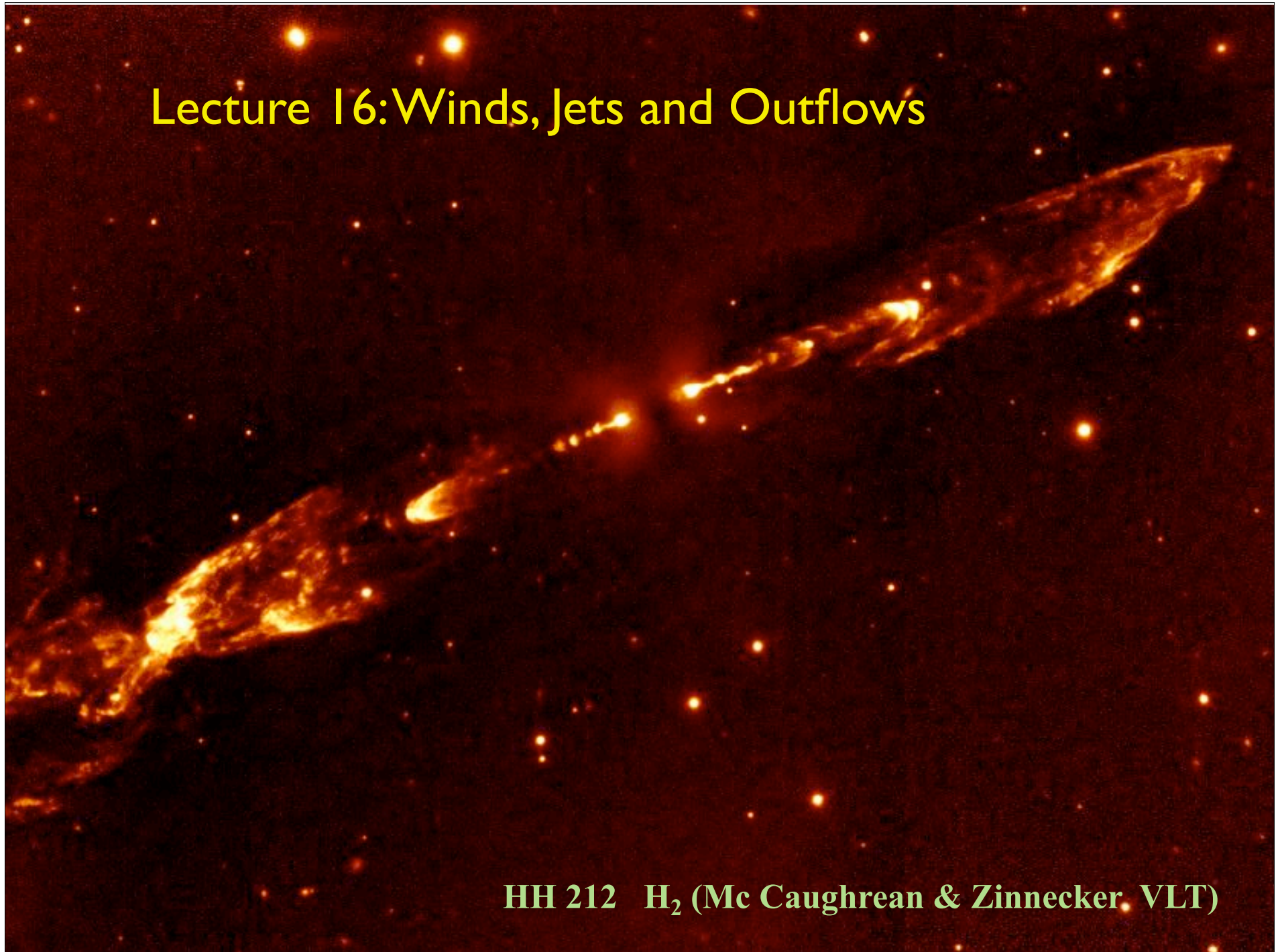


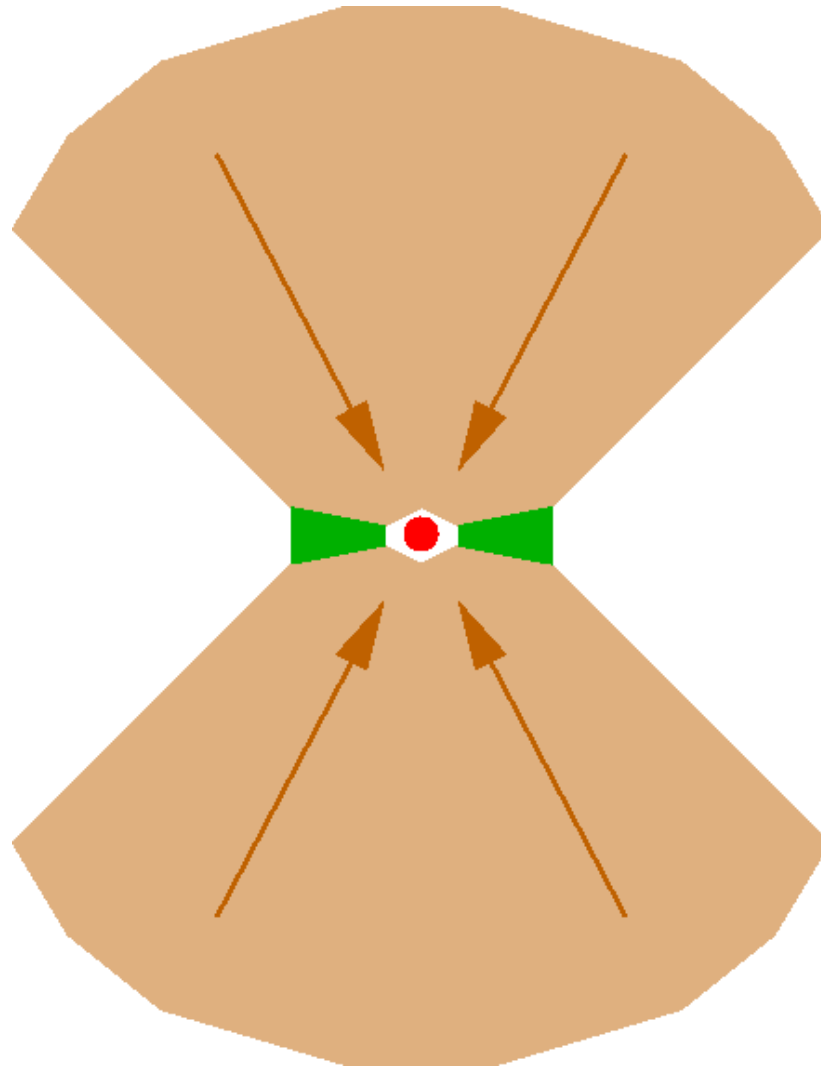
Lecture 16: Winds, Jets and Outflows



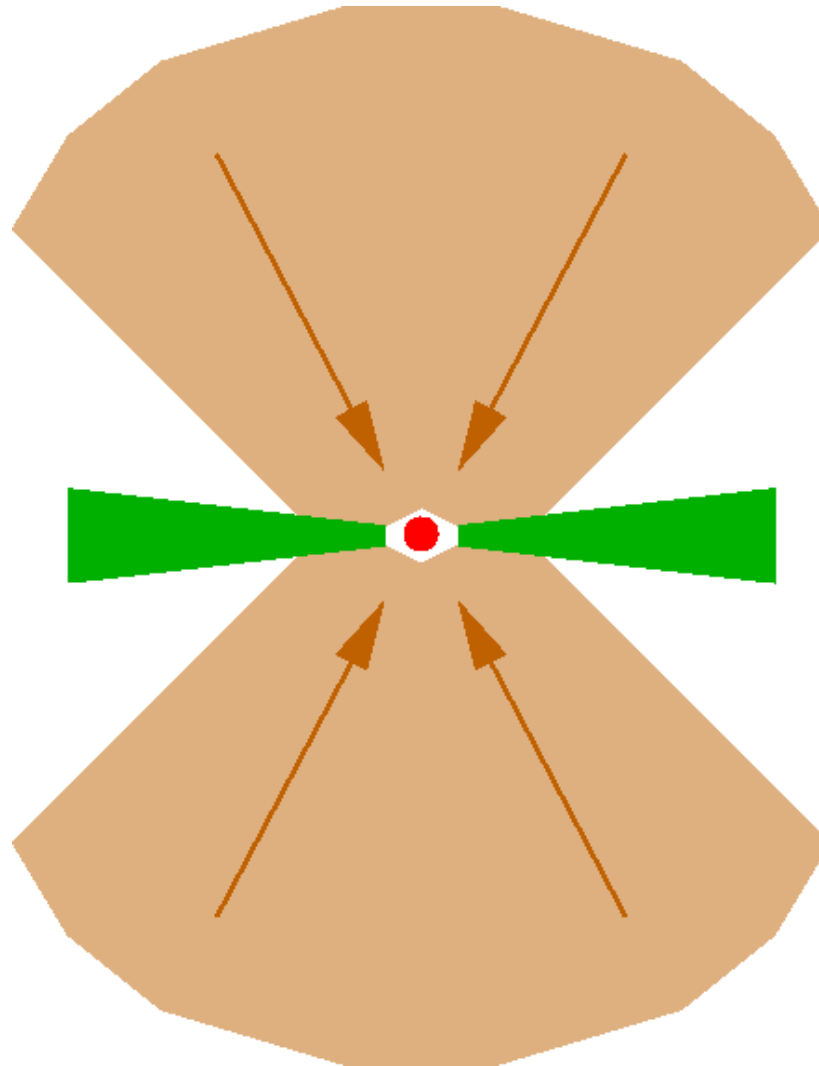
HH 212 H₂ (Mc Caughrean & Zinnecker, VLT)

Losing Material from the Outer Disk Through Photoevaporation

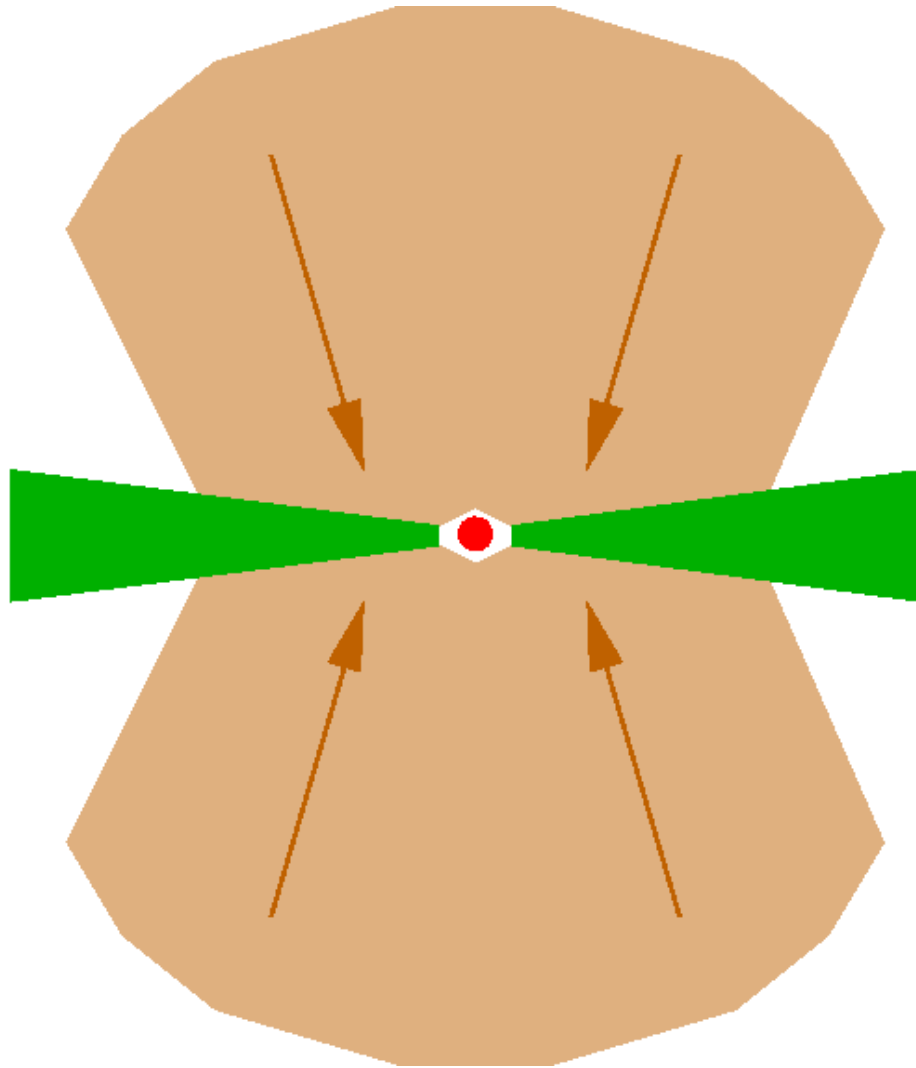
Formation & viscous spreading of disk



Formation & viscous spreading of disk

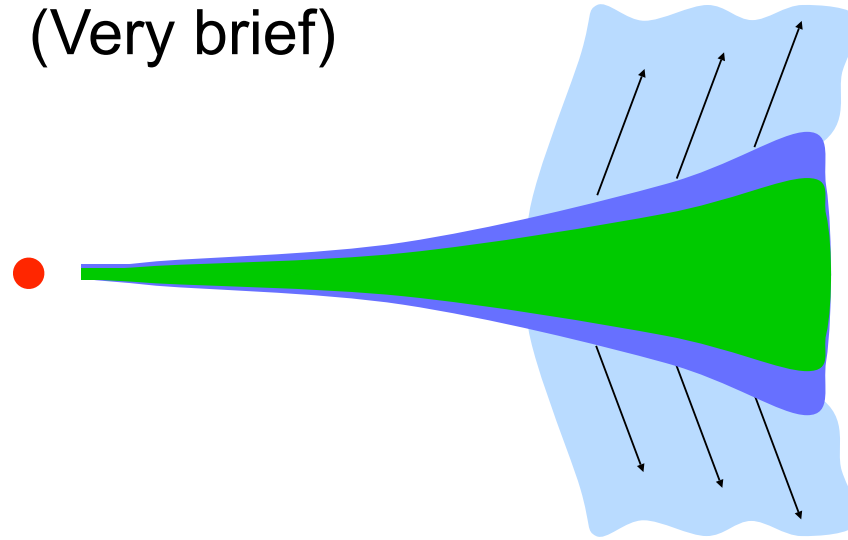


Formation & viscous spreading of disk



Photoevaporation of disks

(Very brief)



Ionization of disk surface creates surface layer of hot gas. If this temperature exceeds escape velocity, then surface layer evaporates.

$$v_{\text{esc}} \approx \left(\frac{GM}{r} \right)^{1/2}$$

Evaporation proceeds for radii beyond:

$$r \geq \frac{GM}{c_{\text{SHI}}^2} \equiv r_{\text{gr}}$$

The Edge of The Solar System: Evaporation of Disks by UV Radiation



Center of Orion
Nebula

Hot O and B-type
stars produce
powerful UV
radiation field.

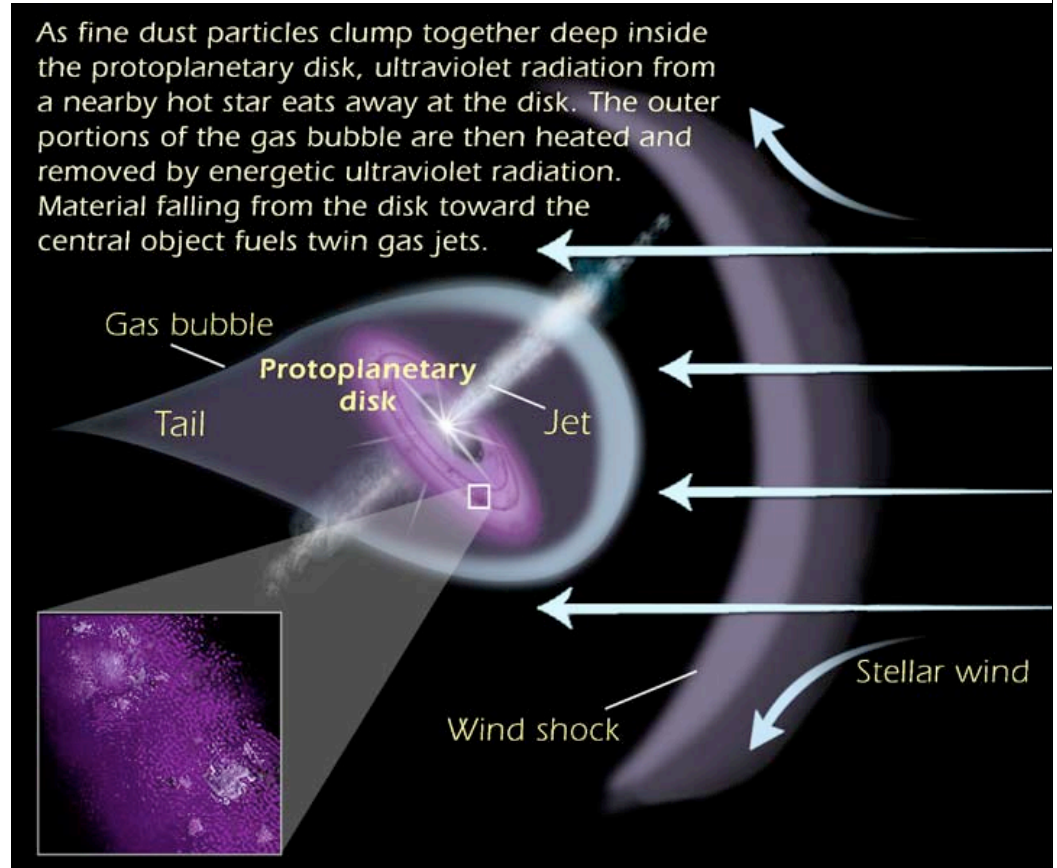
Young disk bathed in
UV light.

Why is there an Edge to the Solar System: Evaporation of Disks by UV Radiation



Protoplanetary Disks in the Orion Nebula HST • WFPC2

NASA, J. Bally (University of Colorado), H. Throop (SWRI),
and C.R. O'Dell (Vanderbilt University) • STScI-PRC01-13



Losing Material from the Inner Disk through Accretion and Outflow

Magnetospheric accretion

Free-fall and accretion shock

From r_A down to star: matter is in supersonic free-fall.

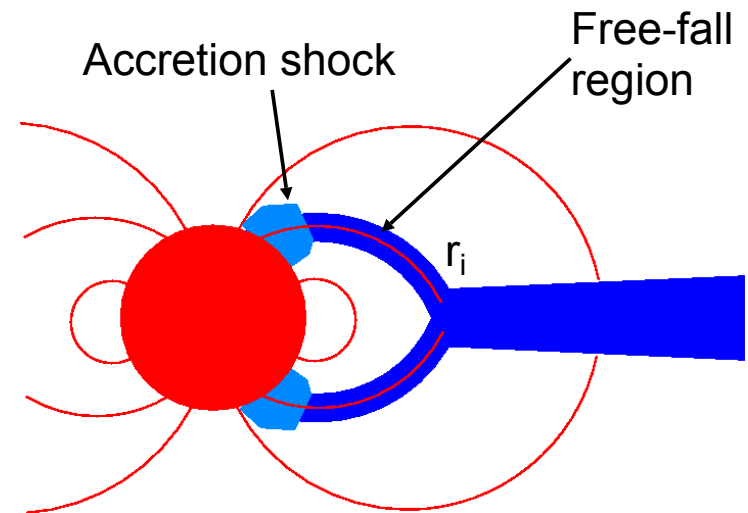
Near the star the matter gets to a halt in a stand-off shock.

Shock velocity:

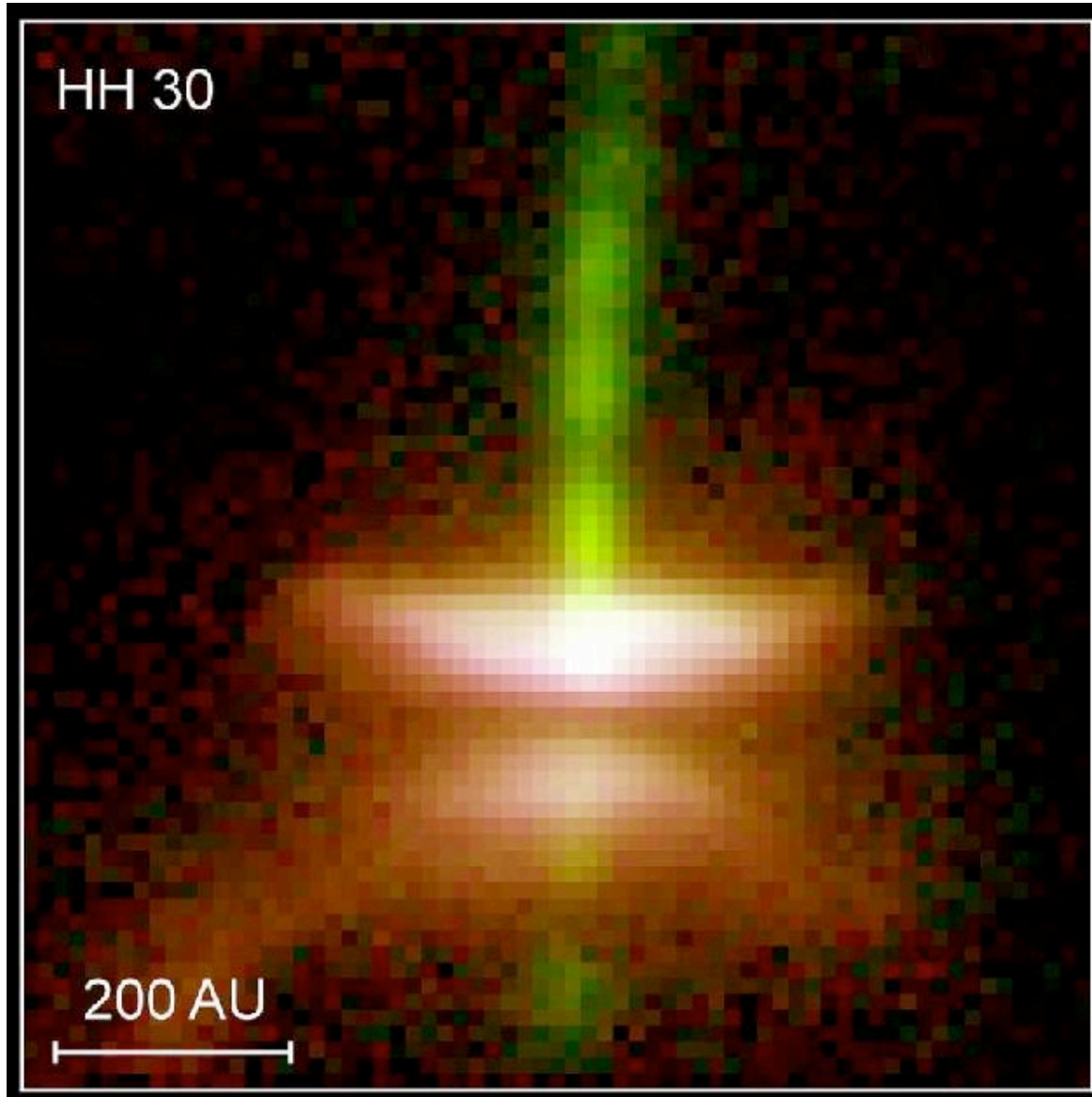
$$v_s = \sqrt{\frac{2GM}{r_*}} \sqrt{1 - \frac{r_*}{r_i}}$$

Dissipated energy (=accretion luminosity from shock):

$$L_{\text{accr}} = \left(1 - \frac{r_*}{r_i}\right) \frac{G\dot{M}M}{r_*}$$



Bipolar outflows

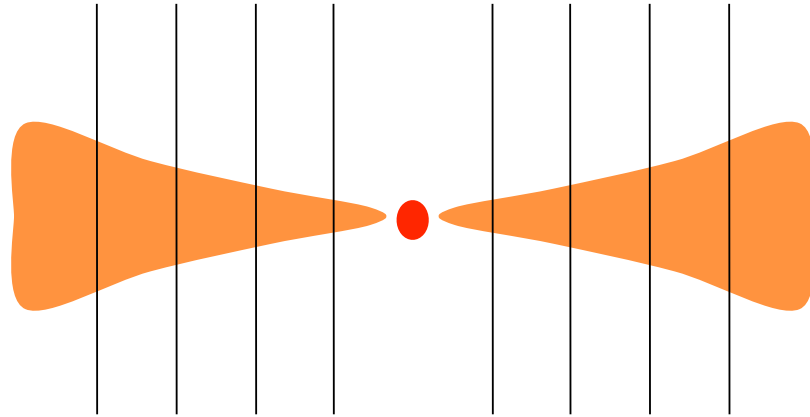


Jets originate from inner regions of protoplanetary disks

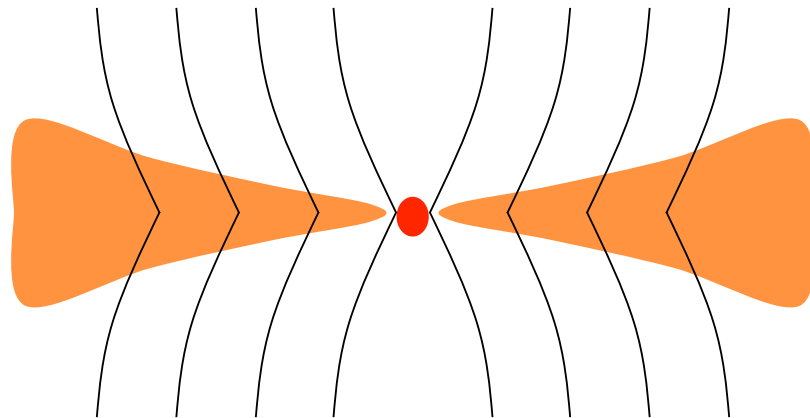
Hubble Space Telescope image

Magnetically threaded disks

Suppose disk is treaded by magnetic field:



Inward motion of gas in disk drags field inward:

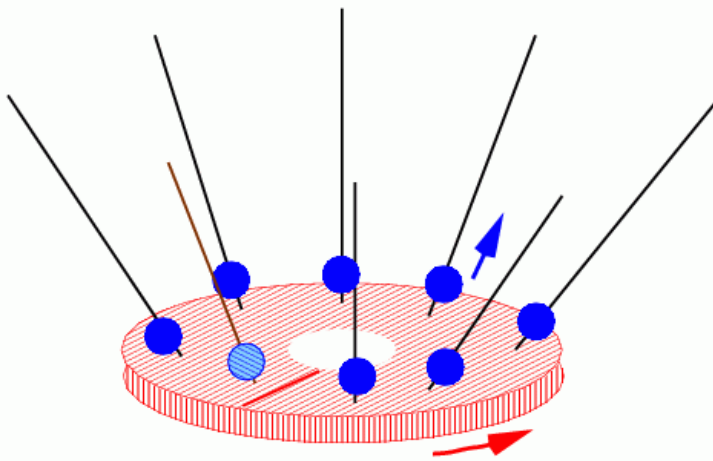


B-field aquires angle with disk

Disk winds

Slingshot effect. Blandford & Payne (1982)

(courtesy:
C. Fendt)



Use *cylindrical*
coordinates r, z

Gravitational potential:

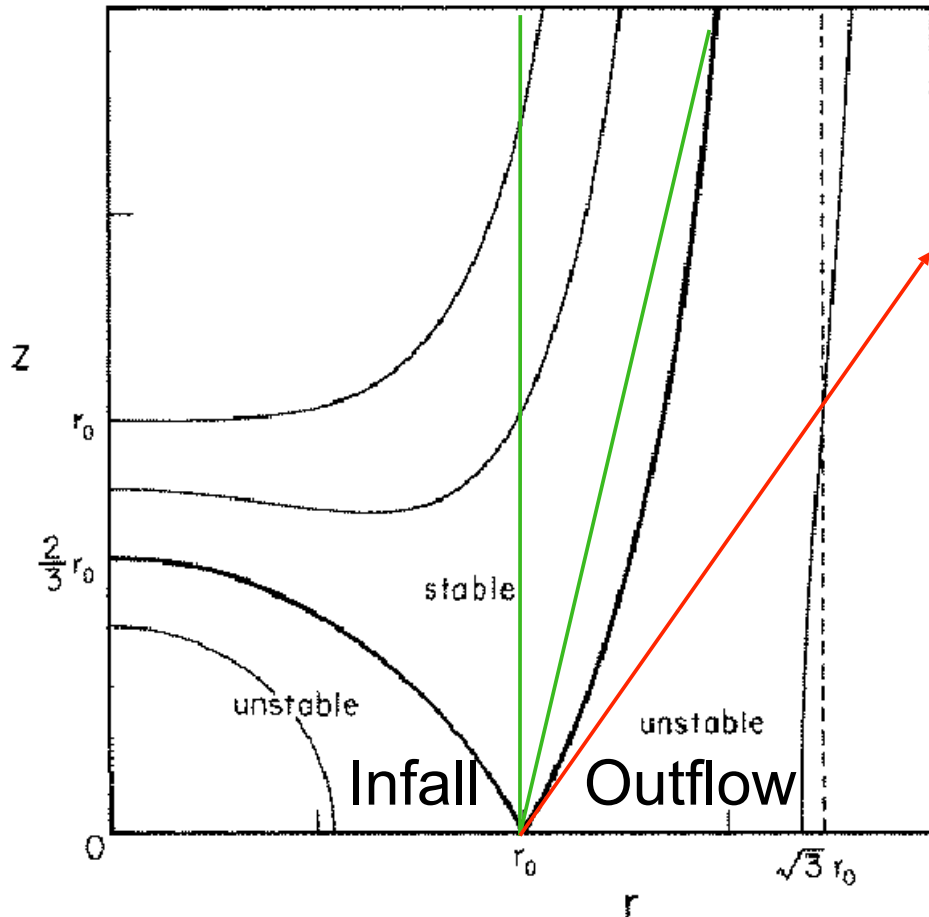
$$\Phi = -\frac{GM}{\sqrt{r^2 + z^2}}$$

Effective gravitational
potential along field line (incl.
slingshot effect):

$$\Phi = -\frac{GM}{r_0} \left[\frac{1}{2} \left(\frac{r}{r_0} \right)^2 + \frac{r_0}{\sqrt{r^2 + z^2}} \right]$$

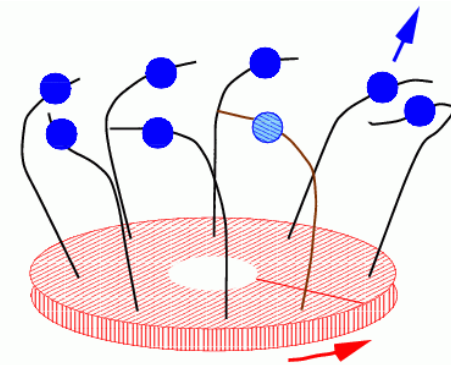
Disk winds

Blandford & Payne (1982)



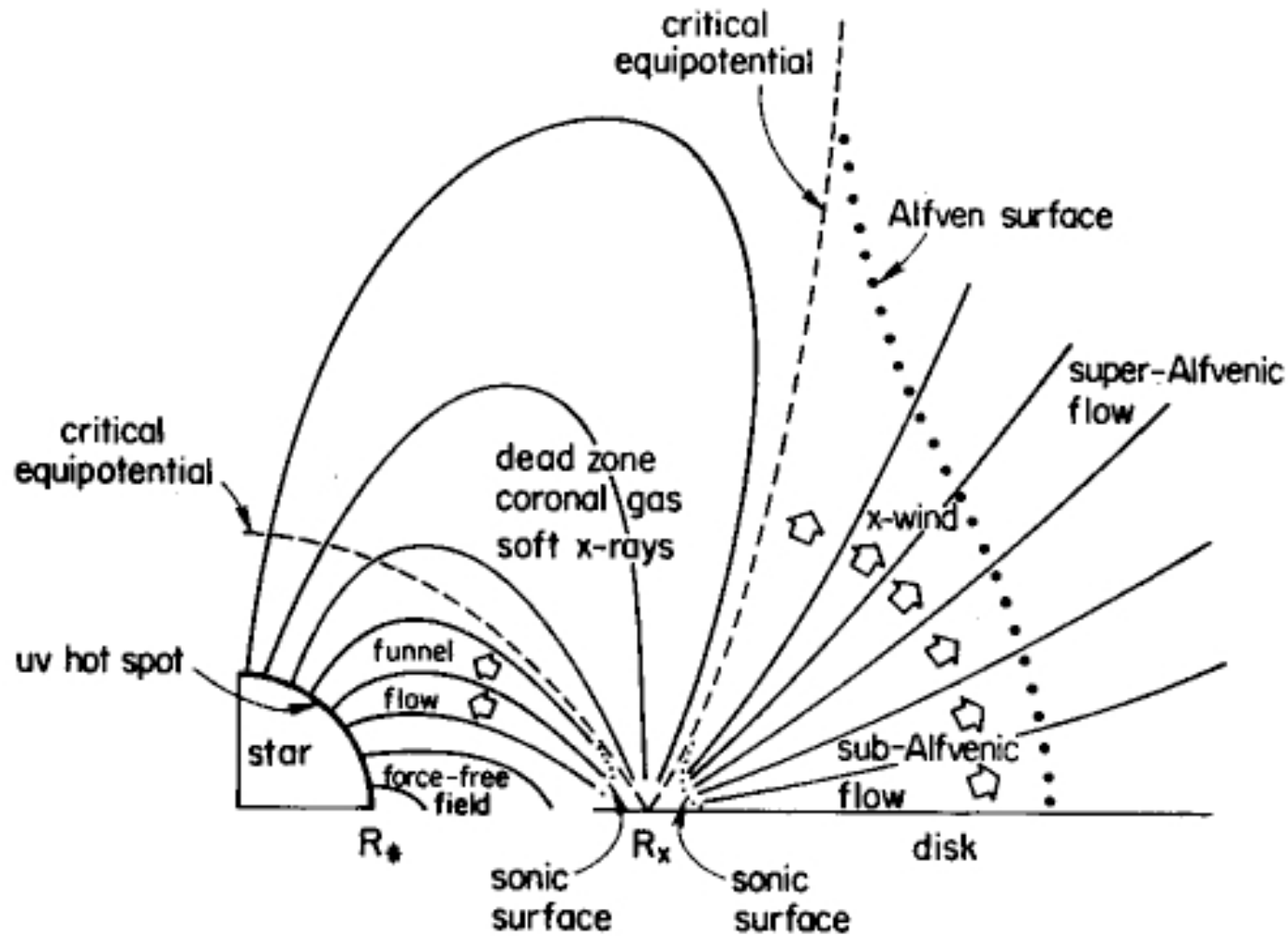
$$\Phi = -\frac{GM}{r_0} \left[\frac{1}{2} \left(\frac{r}{r_0} \right)^2 + \frac{r_0}{\sqrt{r^2 + z^2}} \right]$$

Critical angle: 60 degrees with disk plane. Beyond that: outflow of matter.



Gas will bend field lines

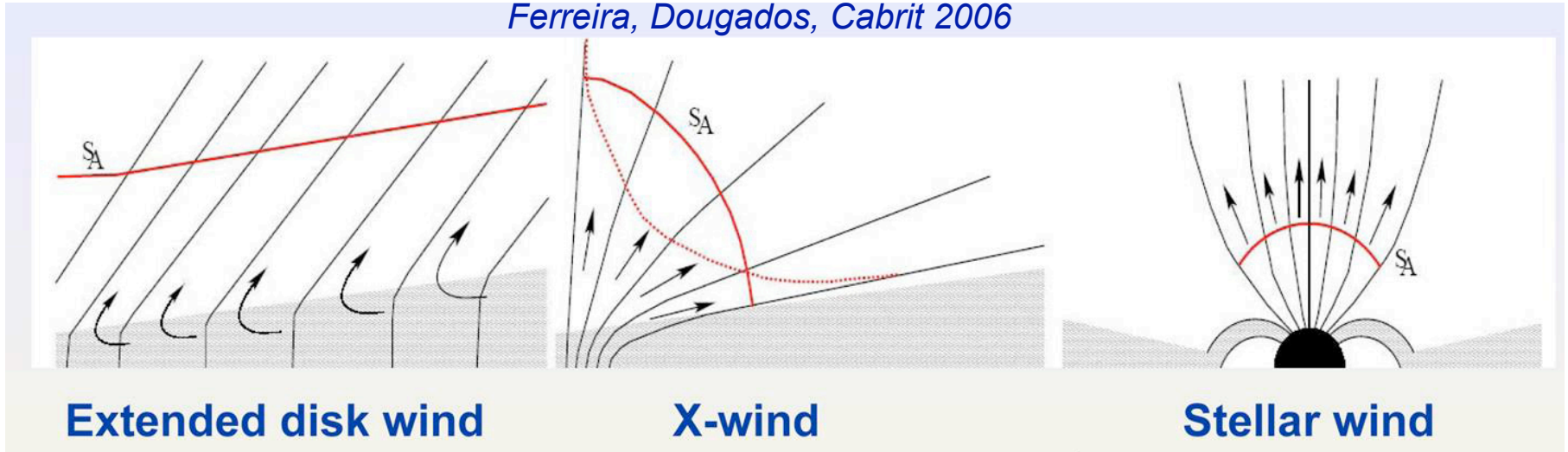
Disk + star: X-wind model of Frank Shu



Shu 1994

Different kinds of Winds

Ferreira, Dougados, Cabrit 2006



Extended disk wind

X-wind

Stellar wind

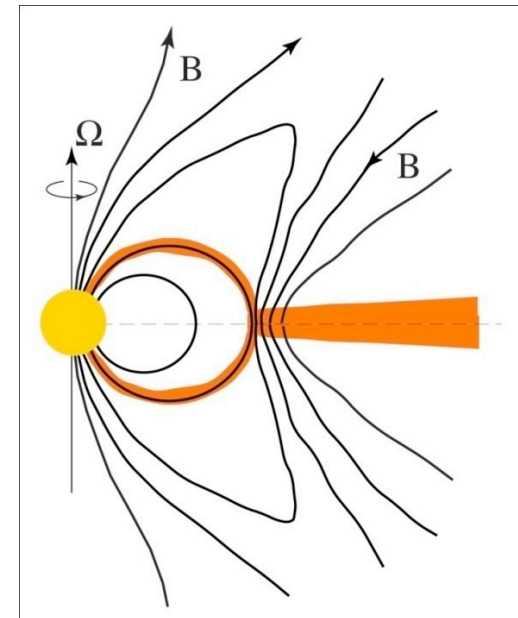
Blandford & Payne 1982
Konigl & Pudritz 2000

Shu et al. 1994

Matt & Pudritz 2005,...



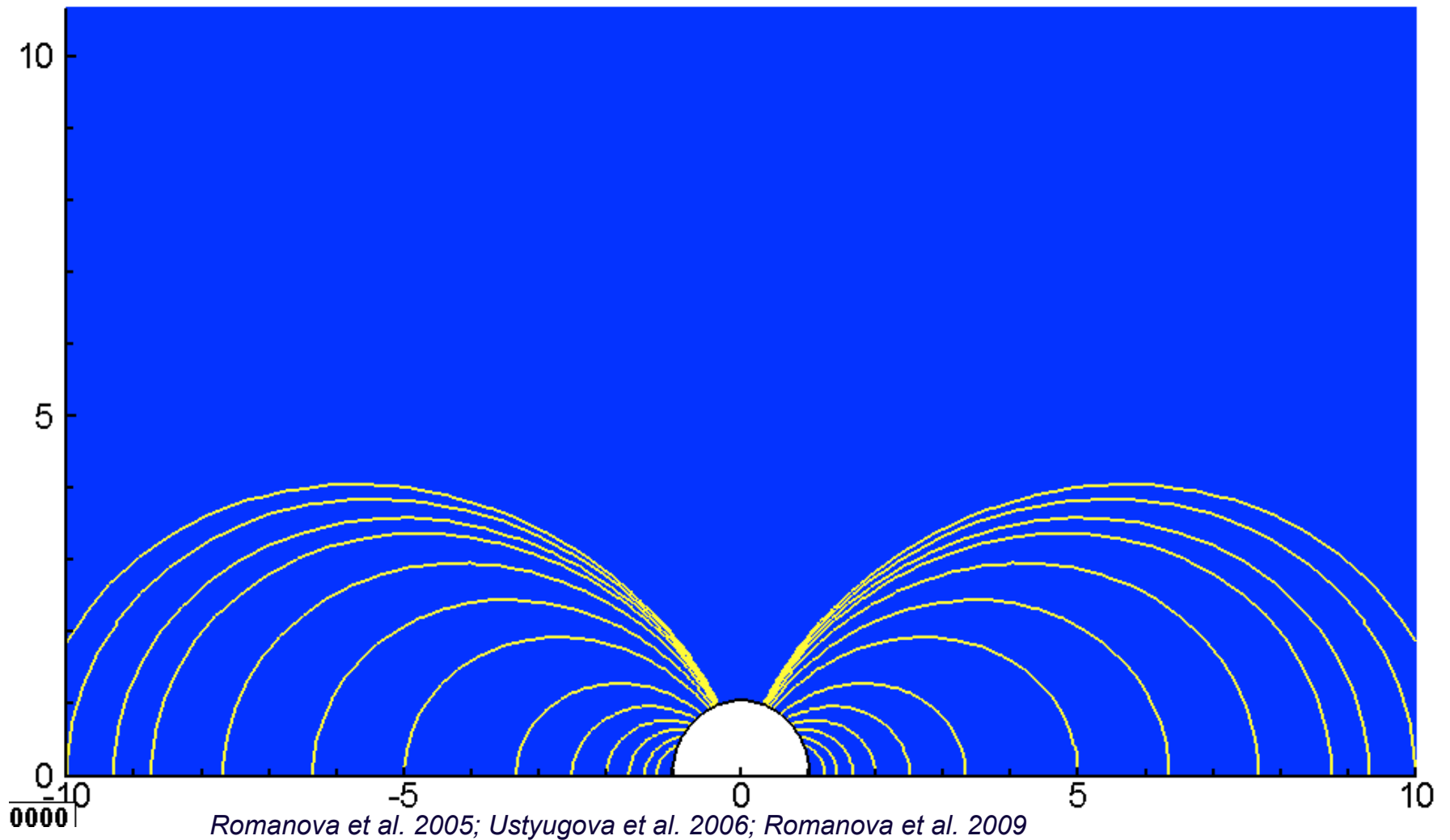
Configuration favorable for outflows



Pirated from talk by
Marina Romanova

Bunching, $\alpha_v > \alpha_d$

Magnetocentrifugal Winds



Jets or Winds?

Wind Blown Cavities

Bipolar Outflows driven by Wind

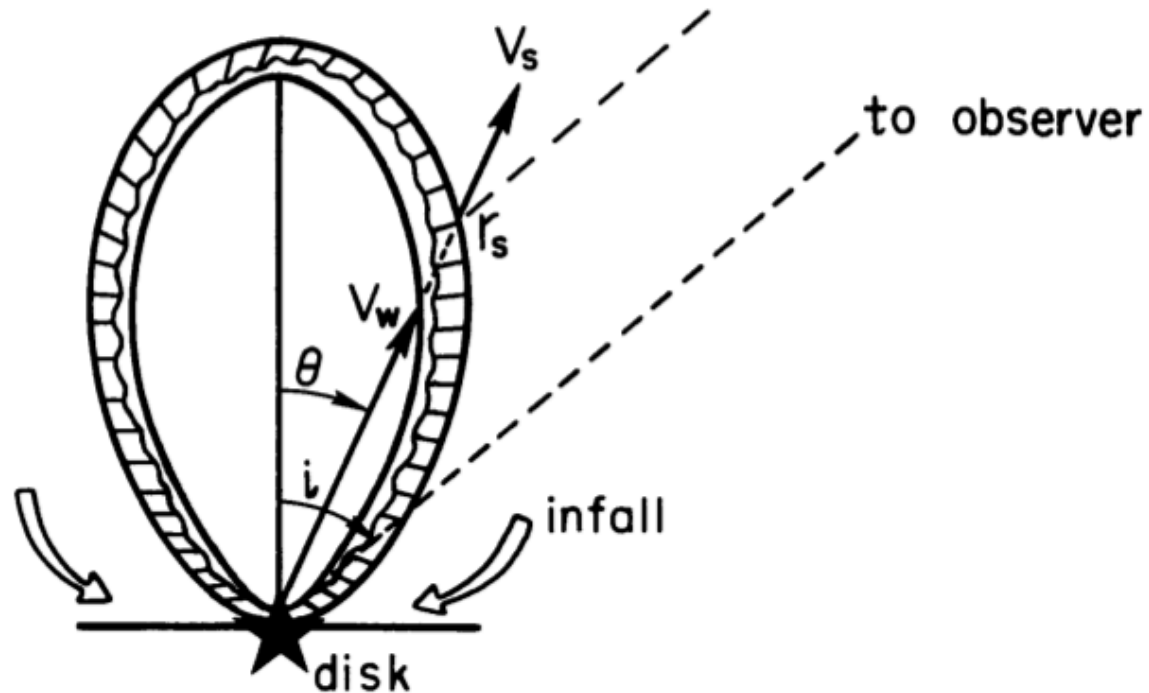


FIG. 1.—Geometry for shell of molecular gas, moving at speed $v_s(\theta)$ at position $r_s(\theta)$, as swept up by a protostellar wind moving at speed $v_w(\theta)$ into a molecular cloud core with the density profile given by eq. (1). The observer views the system at an inclination angle i with respect to the rotation axis of the protostellar disk, and residual infall of cloud material onto the disk occurs in those directions near the equatorial plane not affected by the outflow.

Shu et al. 1991

Wind Blown Bubble

Equations for core:

$$\rho(r, \theta) = \frac{c_s^2}{2\pi G r^2} Q(\mu) \quad (1)$$

$$\int_0^1 Q(\mu) d\mu = 1 \quad (2)$$

$$\dot{M} \approx \frac{c_s^3}{G}, \quad \dot{M}_w = f \dot{M} \quad (3)$$

Equations for wind:

$$P(r, \theta) = \frac{\dot{M}_w v_w}{4\pi} P(\mu) \quad (4)$$

$$\int_0^1 P(\mu) d\mu = 1 \quad (5)$$

Wind Blown Bubble

Assuming momentum conservation but not energy conservation (snowplot), the mass per steradian, M_{sr} , grows

$$\frac{dM_{sr}}{dt} = \frac{c_s^2}{2\pi G} Q(\mu) v_s \quad (6)$$

And the momentum grows by:

$$\frac{d}{dt}(M_{sr} v_s) = \frac{\dot{M}_w v_w}{4\pi} P(\mu) \quad (7)$$

Now we balance momentum change per steradian due to wind with ram pressure per steradian

$$v_s \frac{dM_{sr}}{dt} = \frac{c_s^2}{2\pi G} Q(\mu) v_s^2 = \frac{\dot{M}_w v_w}{4\pi} P(\mu) \quad (8)$$

Wind Blown Bubble

implying

$$v_s = \left(\frac{\dot{M}_w}{2\dot{M}} \right)^{1/2} (c_s v_w)^{1/2} \beta(\mu), \text{ where } \beta(\mu) = \left(\frac{P(\mu)}{Q(\mu)} \right)^{1/2} \quad (9)$$

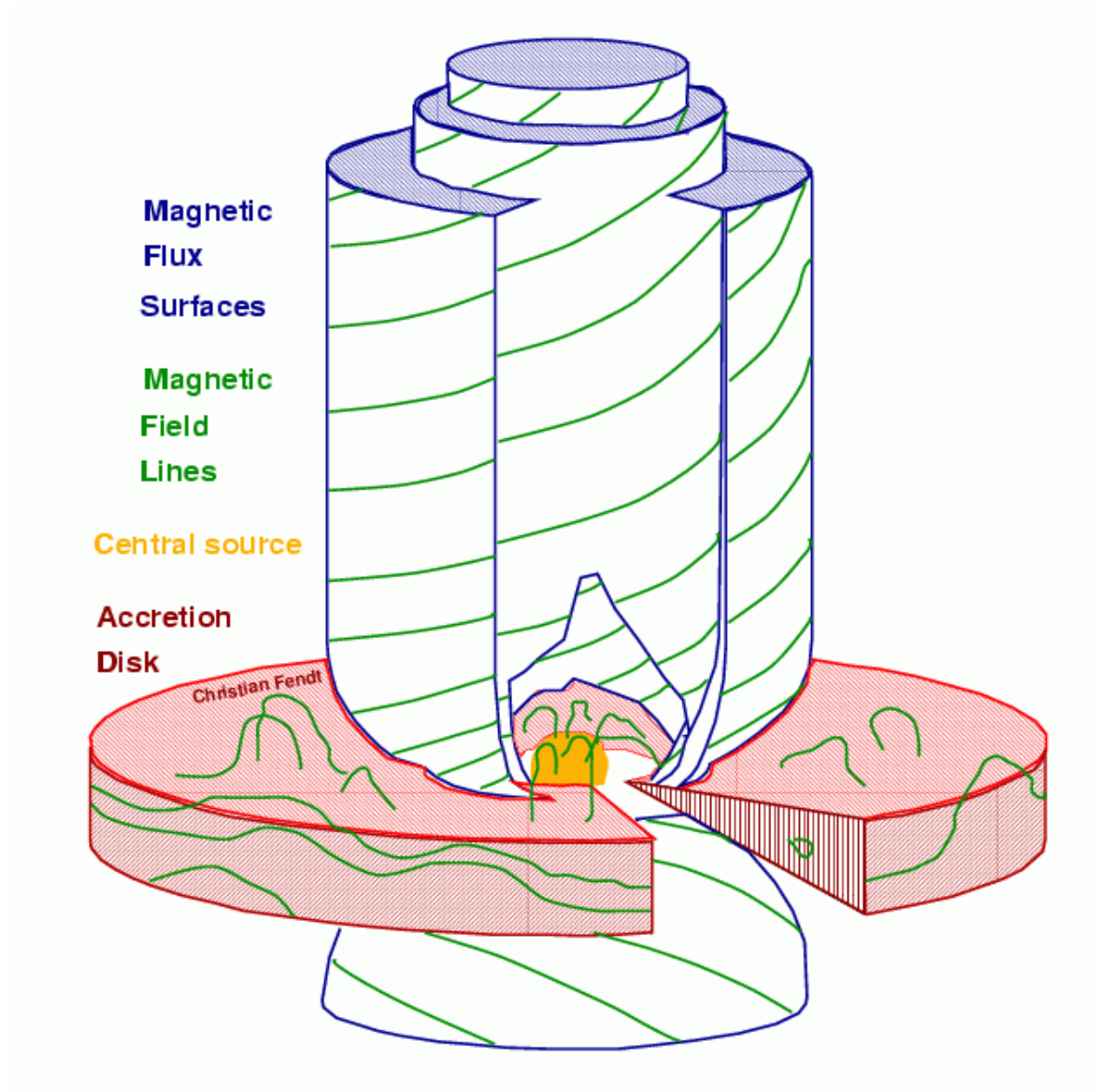
$$r_s = (f/2)^{1/2} (c_s v_w)^{1/2} t \beta(\mu) \quad (10)$$

This gives a "Hubble" law for outflows:

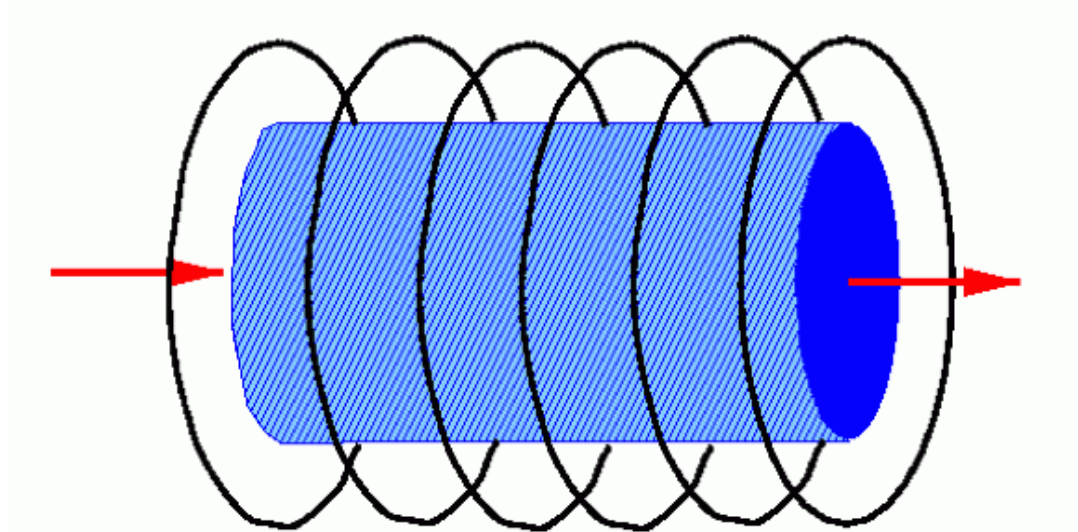
$$v_s = \frac{r_s}{t} \quad (11)$$

Creating Jets

Creating Jets: Magnetic field winding - confinement



Magnetic field winding - confinement



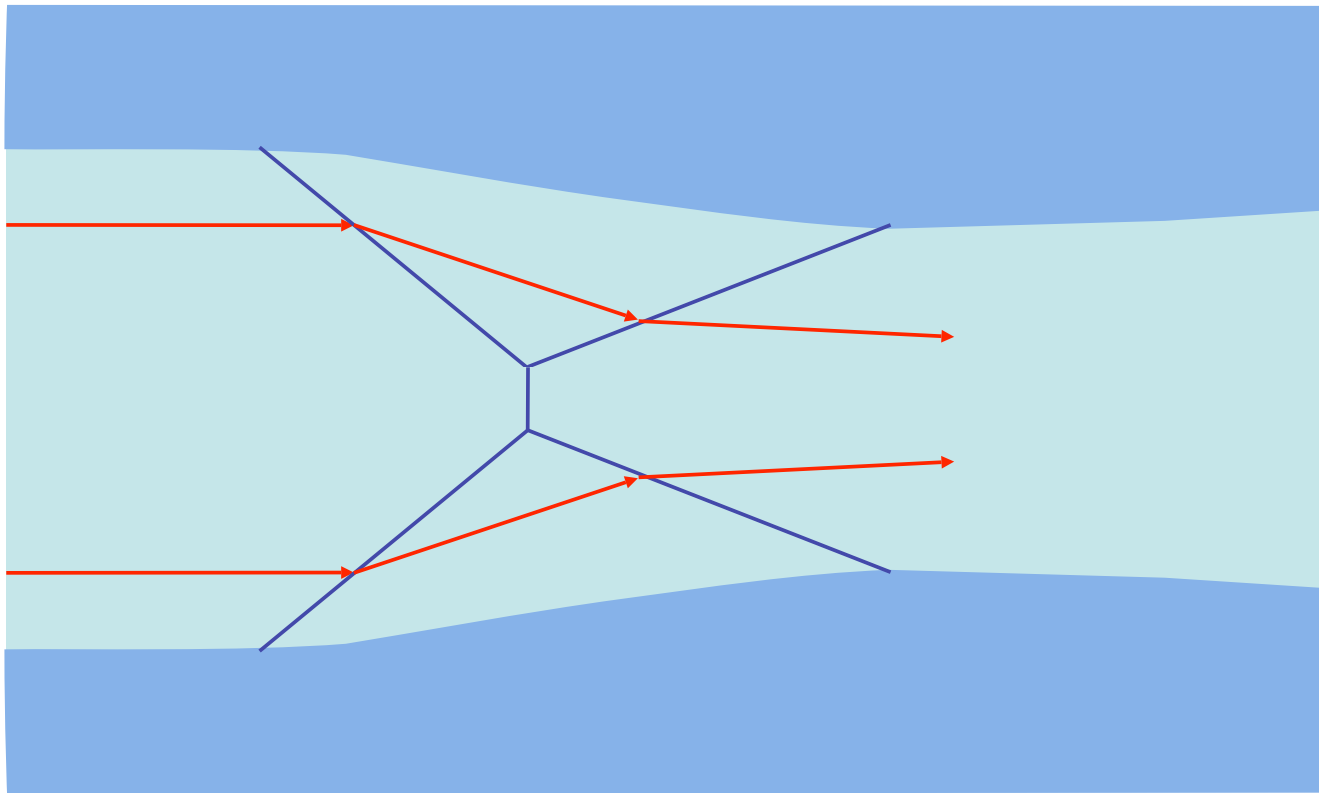
(courtesy:
C. Fendt)

$$\vec{j} = \frac{c}{4\pi} \nabla \times \vec{B}$$

$$\vec{f} = \frac{1}{c} \vec{j} \times \vec{B}$$

Right-hand rule:
force points
inwards

Hydrodynamic confinement in jet:



Shock only reduces the velocity component perpendicular to shock front. Therefore obliquely shocked gas is deflected toward the shock plane.

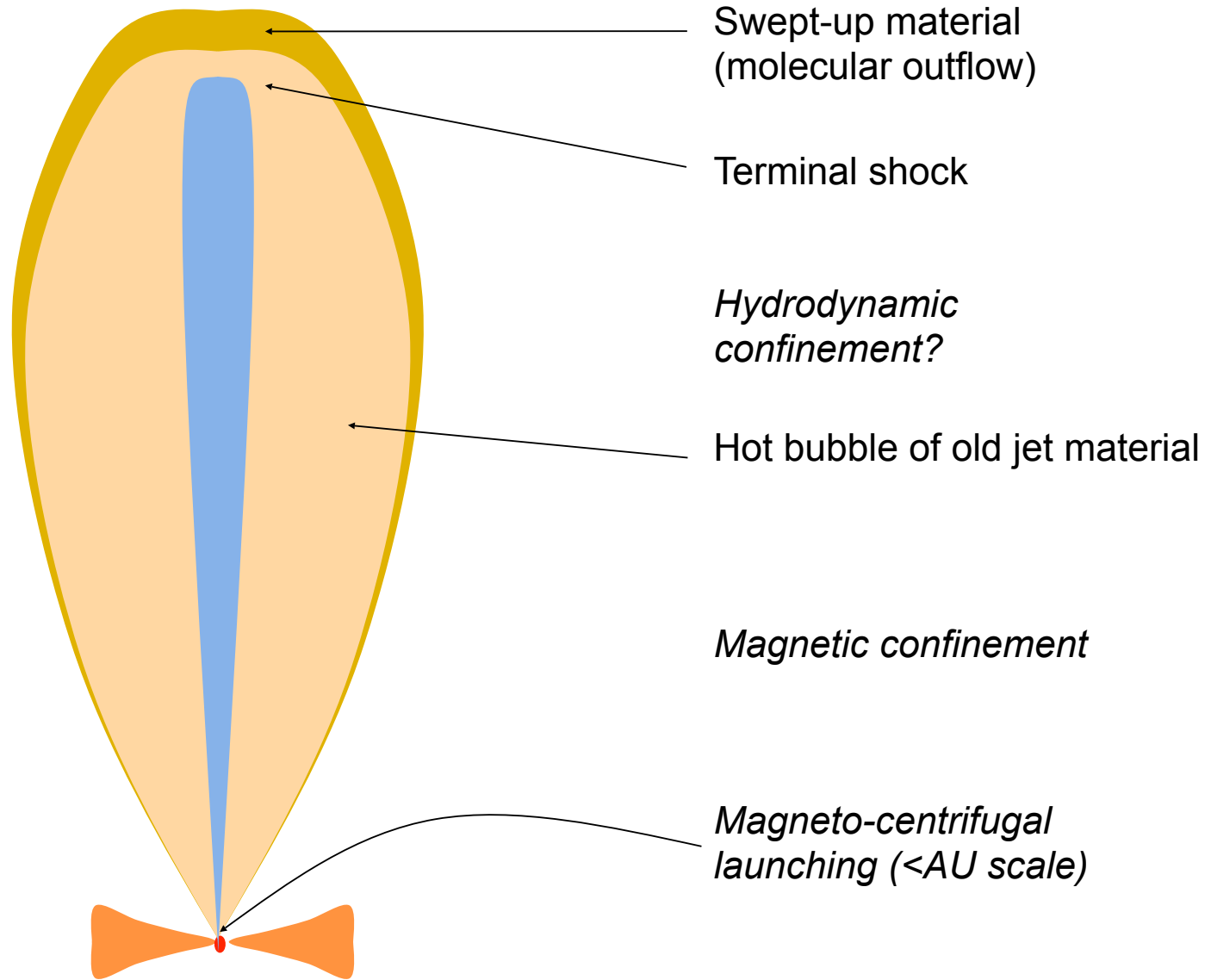
Hydrodynamic confinement in jet:



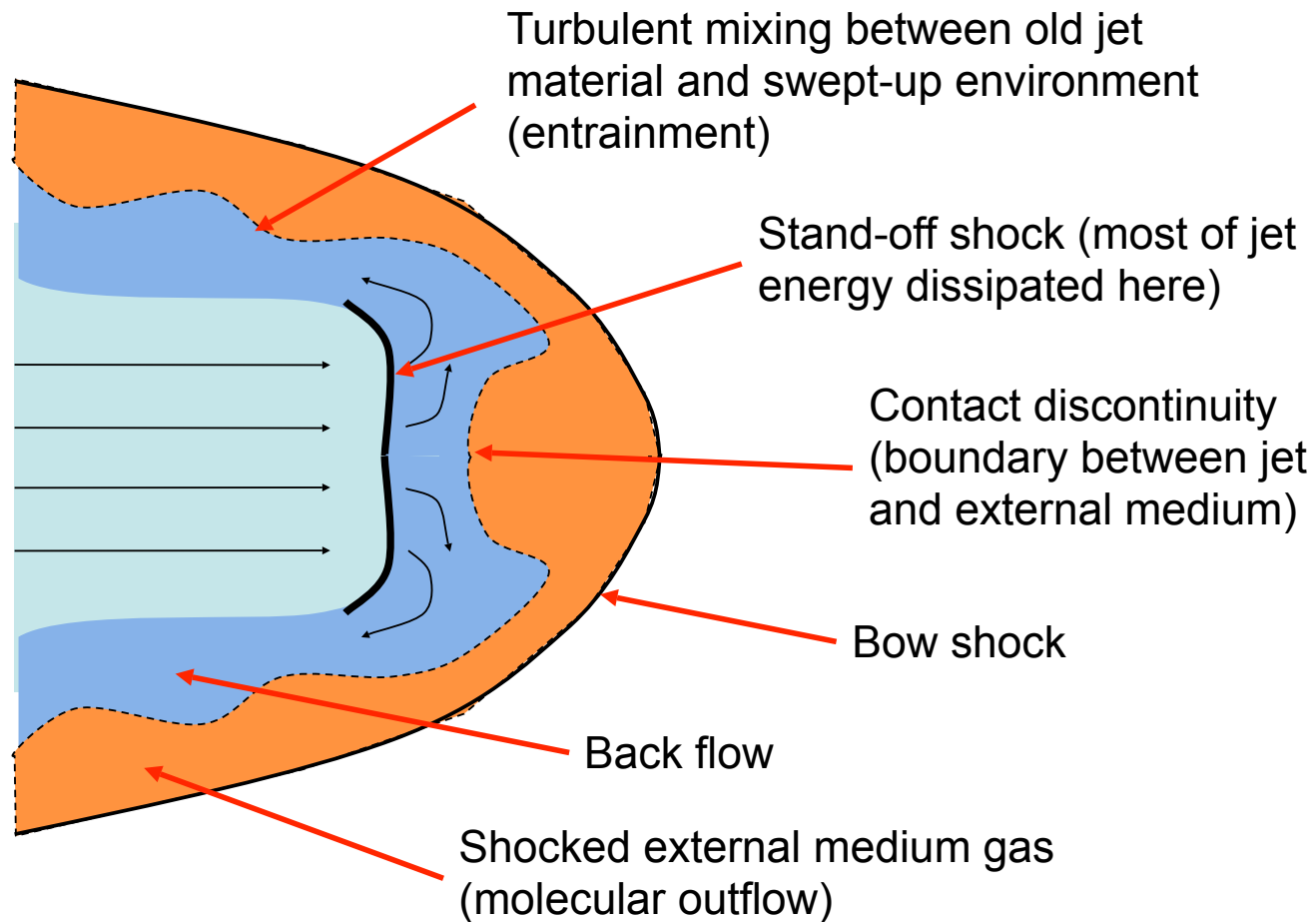
Dryden Flight Research Center EC93-03092-7 Photographed 1994
SR-71 Ship #1



Bipolar outflows driven by Jets



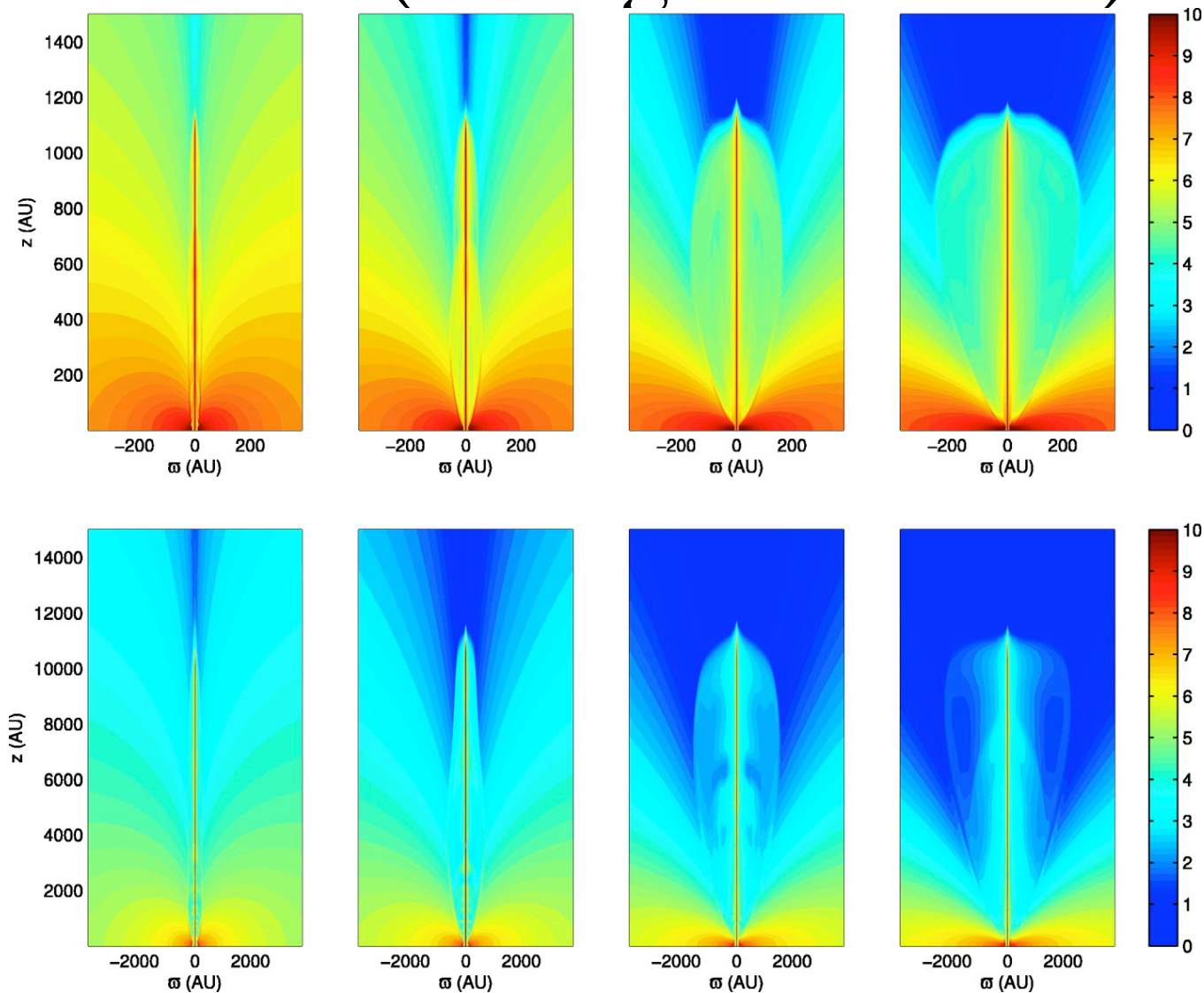
Head of the jet:



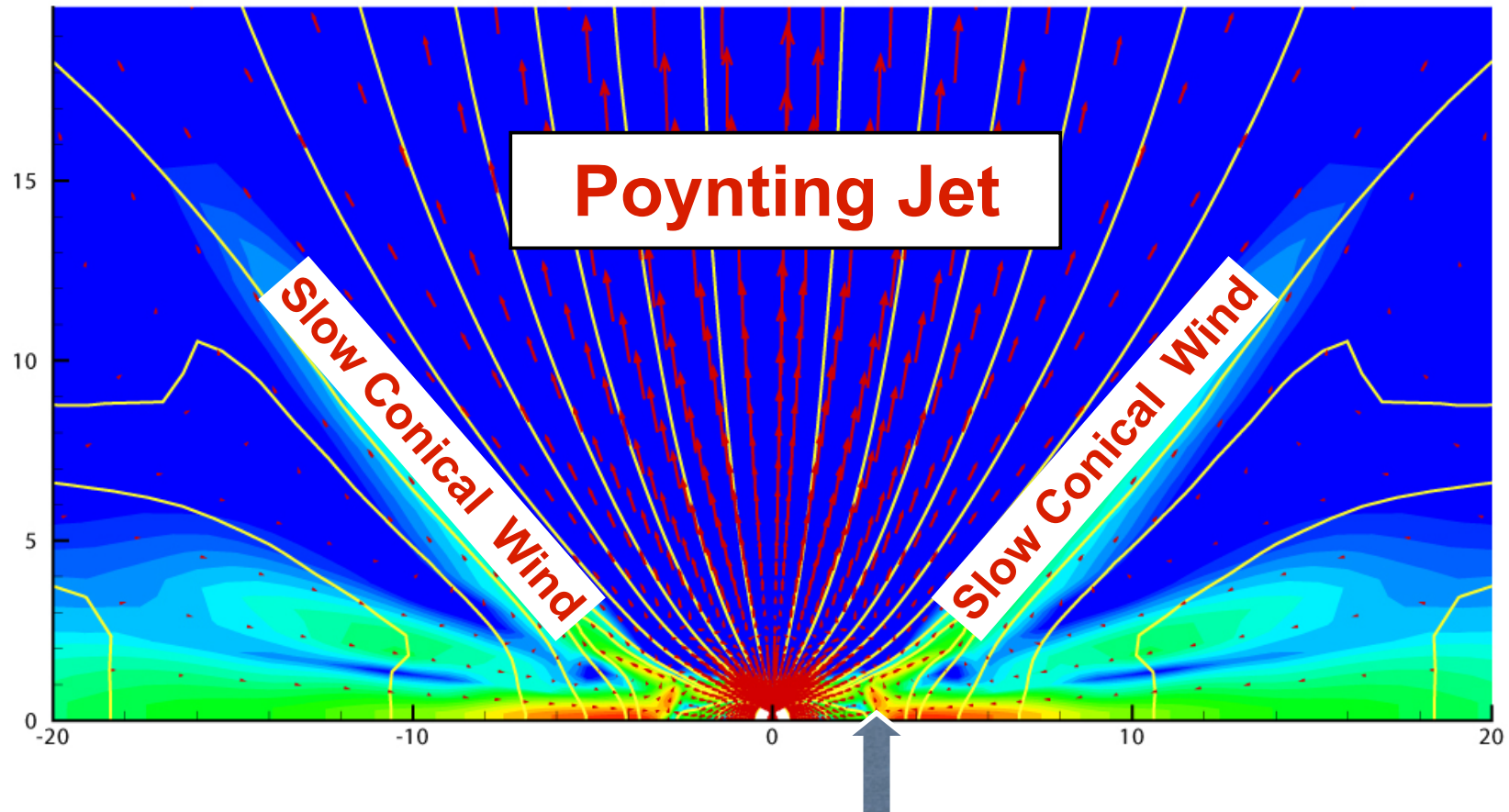
Jet flow much faster than propagation of bow shock.
Jet material much more tenuous than external medium

Most Likely a Combination of Both

A Unified Models of Jets and Winds (Shang et al 2006)



Rapidly-rotating stars: Propeller regime

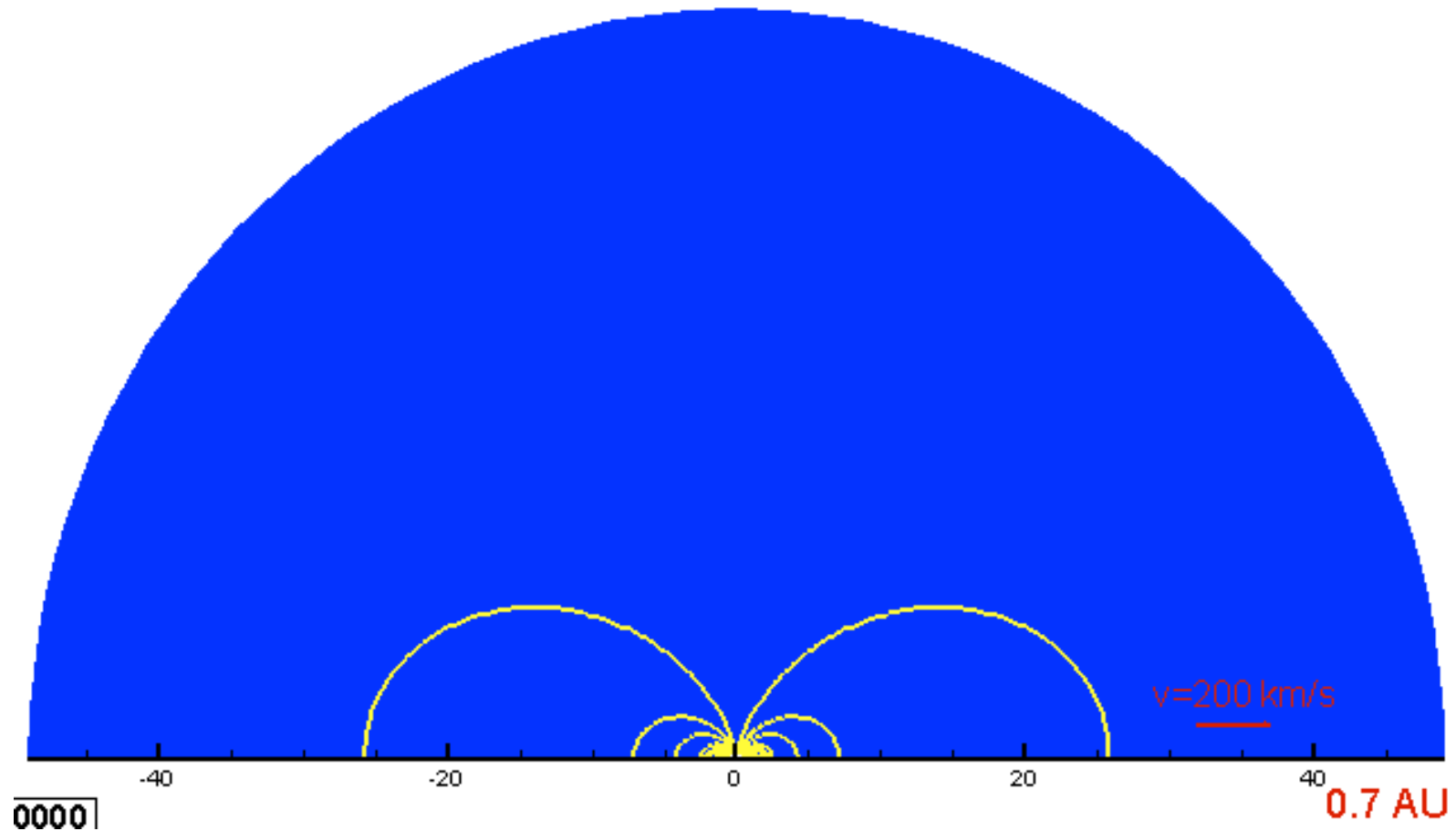


- Two-component outflow forms
- Conical winds carry most of matter outwards
- Poynting jet carries energy and ang. momentum

Romanova et al. 2005; Ustyugova et al. 2006; Romanova et al. 2009

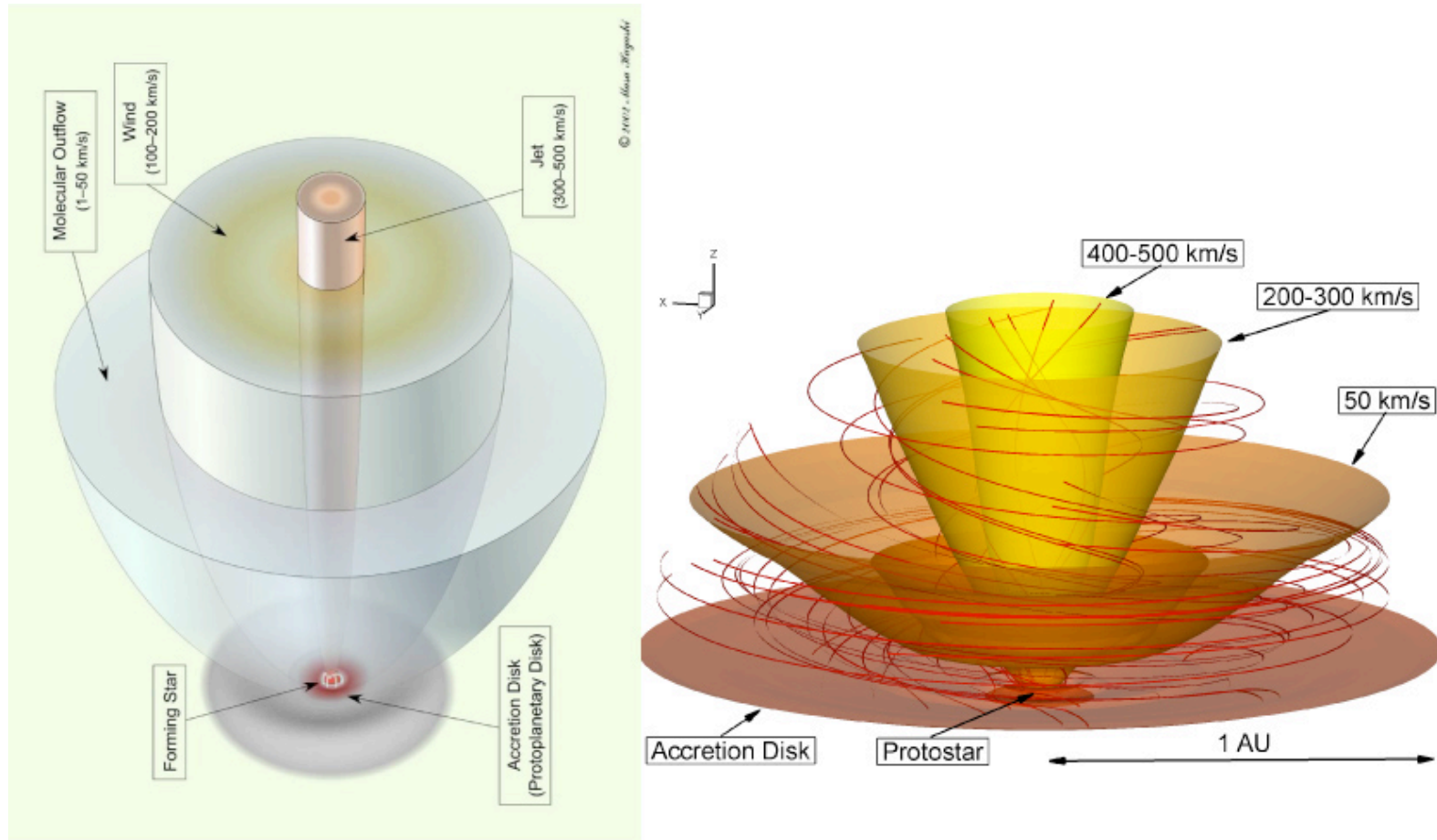
The Propeller Regime

Disk radius $>$ Corotation Axis:
Magnetic field rotating faster than disk



Ustyugova et al. 2006

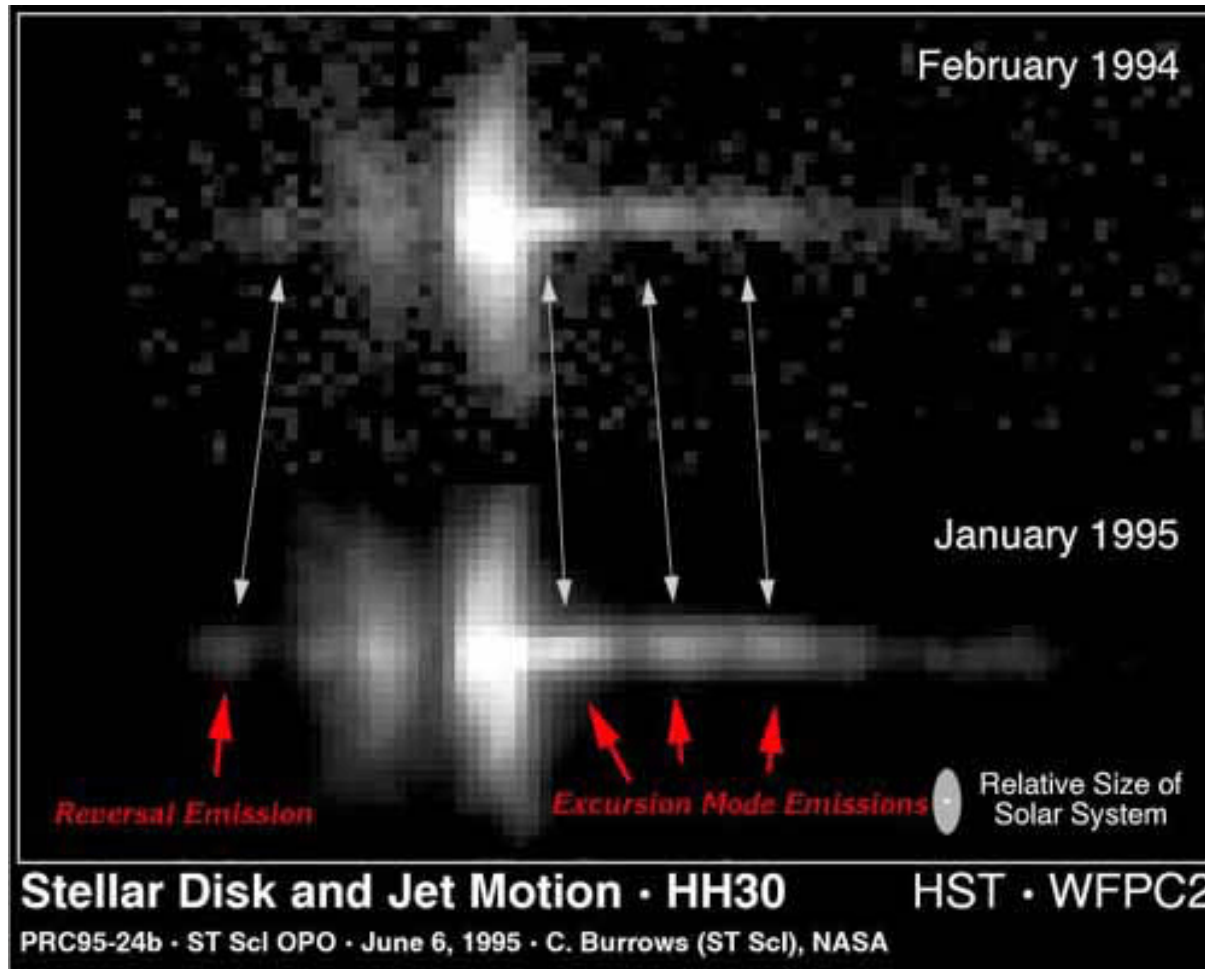
Outflows at the Propeller Stage: Conical Winds + Axial Jet



A star spins-down due to axial magnetic jet

Pirated from talk by Marina Romanova

Observed knot movement



Observations of Jets and Winds

Herbig-Haro Objects

Discovered independently by George Herbig and Guillermo Haro in 1950s

Small knots of nebulosity in dark clouds

Displayed lines of hydrogen and forbidden lines of [OI], [NII] and [SII].

Now known to be shock ionized nebulae.

More than 400 Herbig Haro (HH) objects are known.

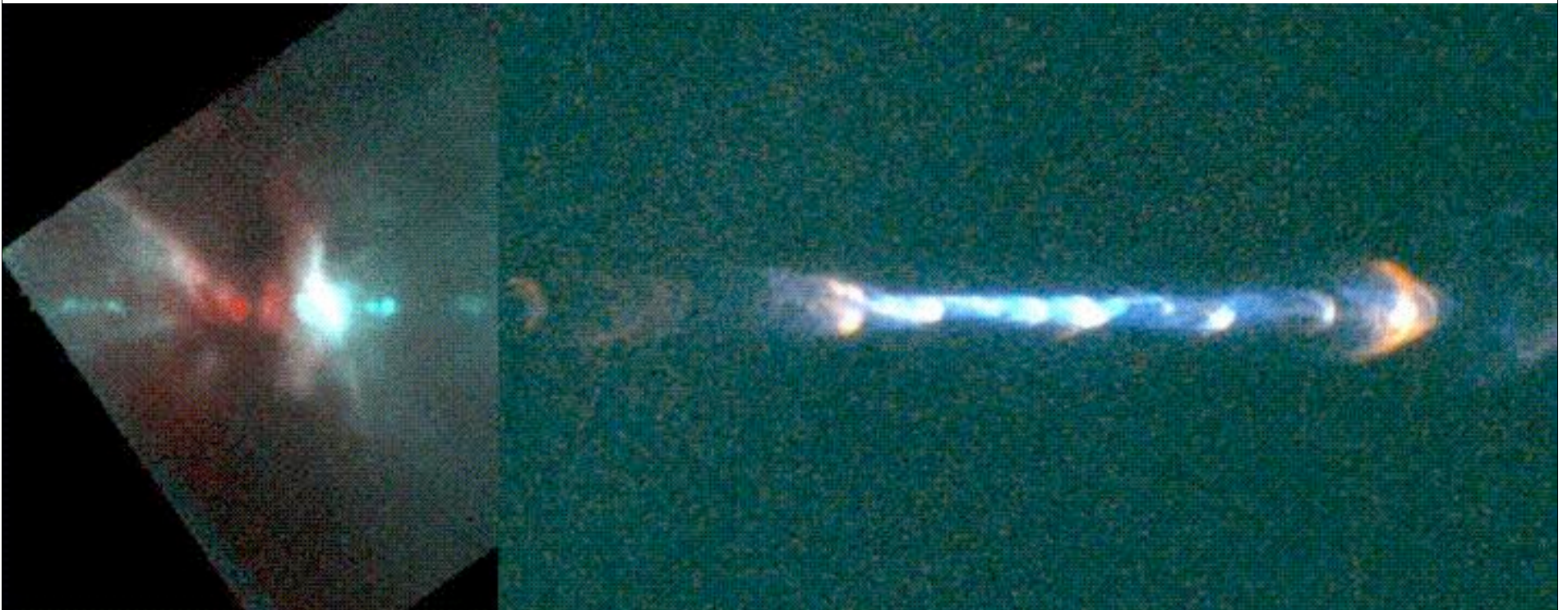
Only trace a small fraction of the outflowing gas

HH 111

Knots are probably internal shocks, where faster knots are crashing into slower knots

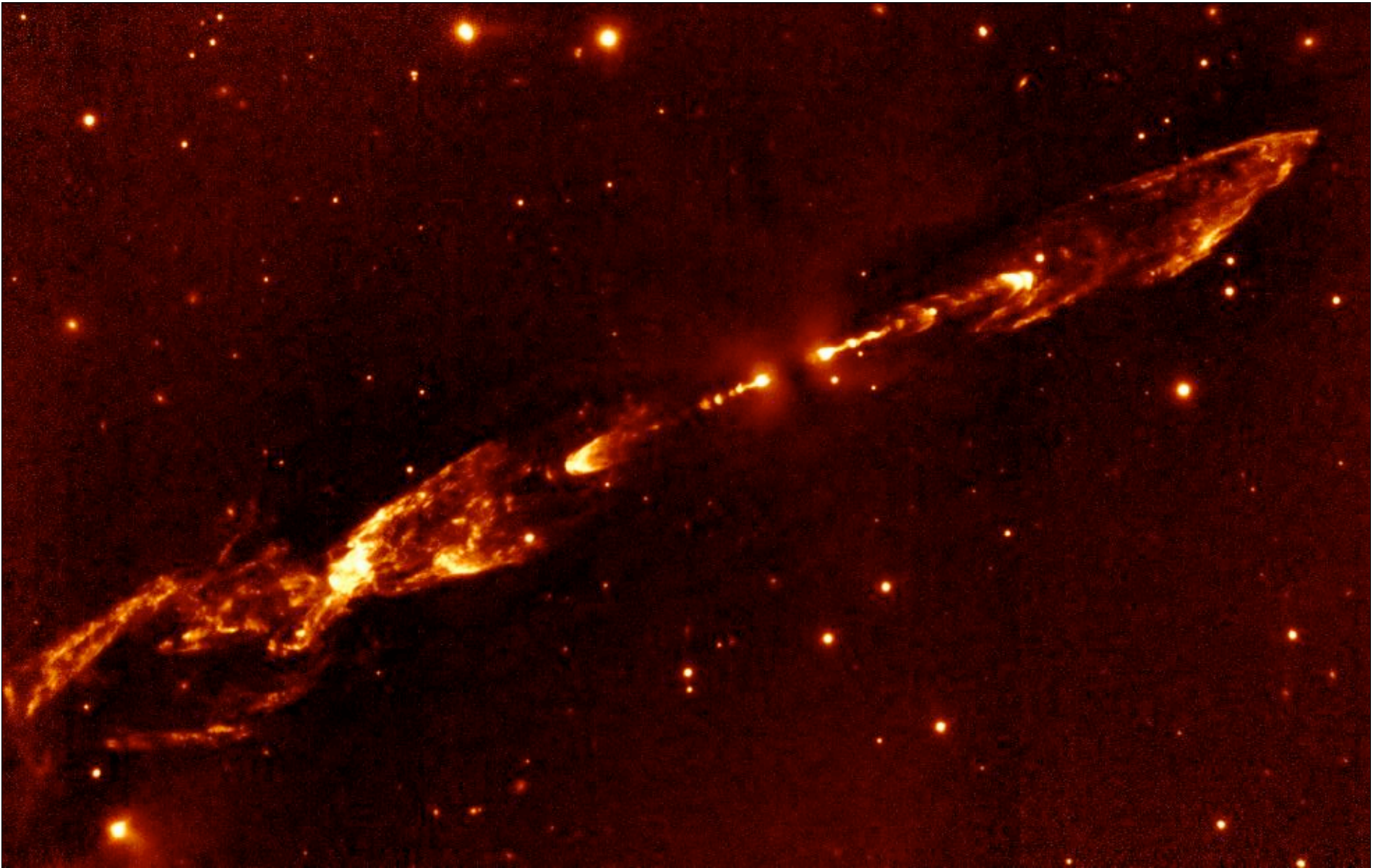
[Fe II] + K

Ha + [SII]

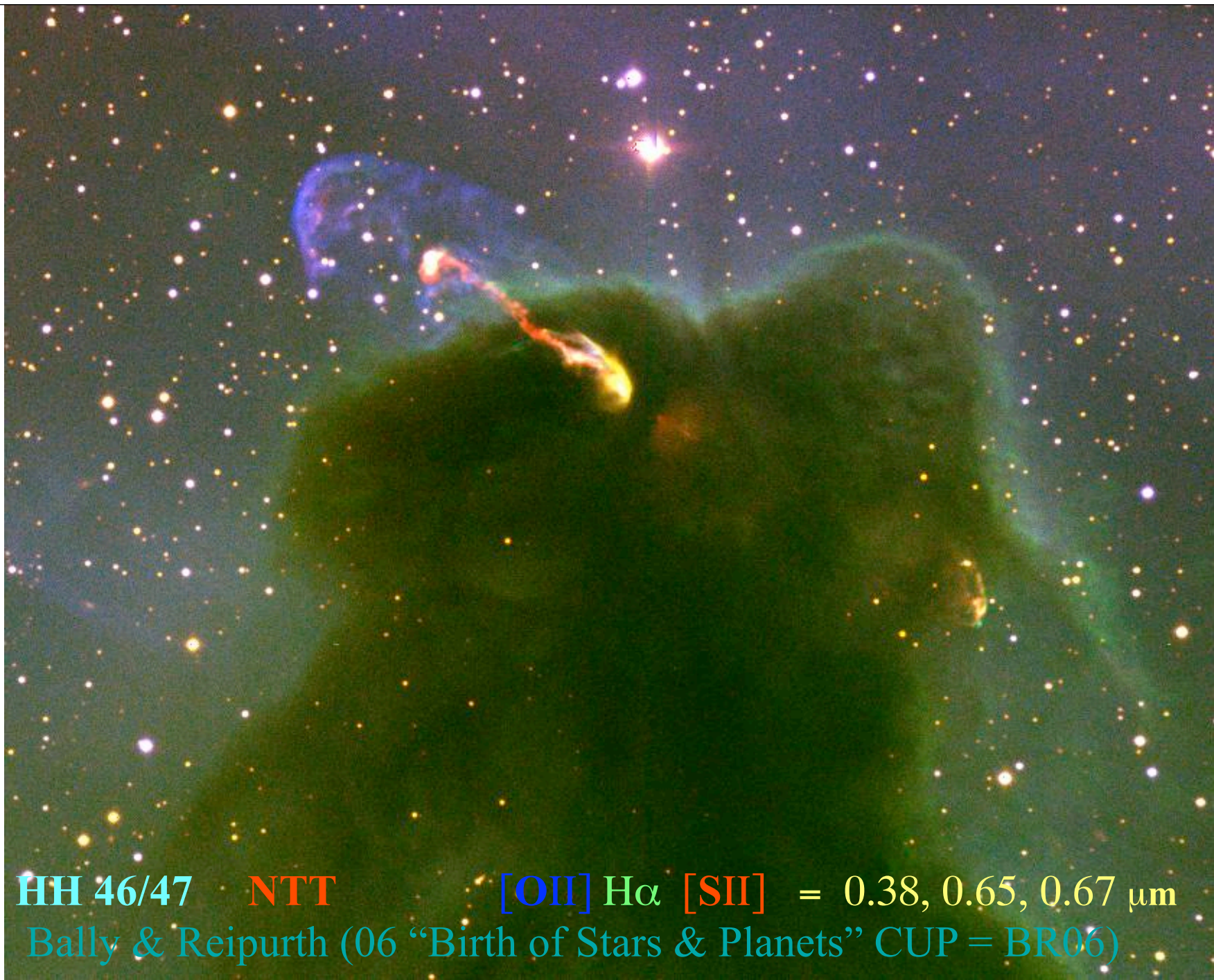


NICMOS

WFPC2



HH 212 H₂ (Mc Caughrean & Zinnecker VLT)



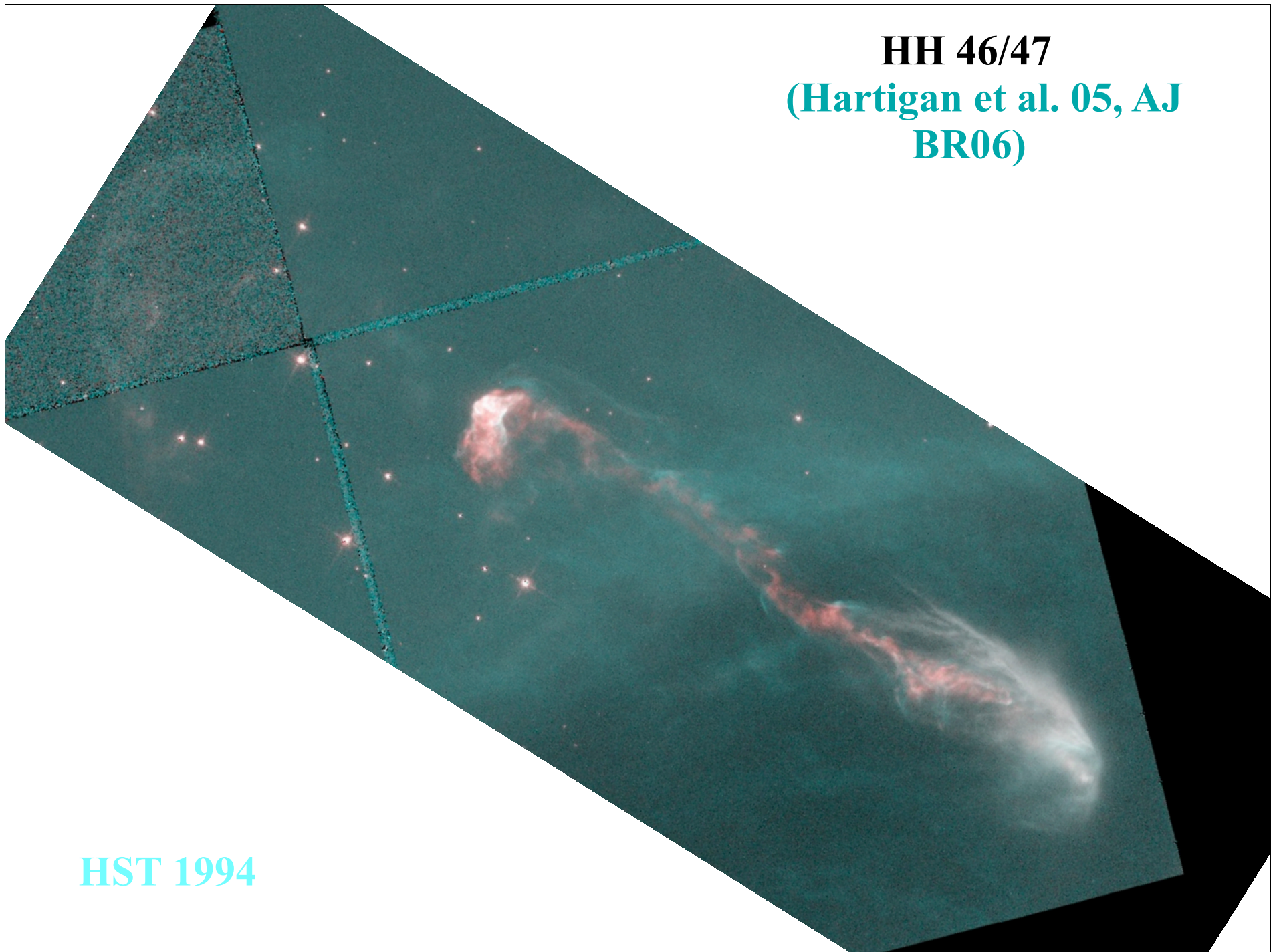
HH 46/47 · **NTT** · **[OII]** $H\alpha$ **[SII]** = 0.38, 0.65, 0.67 μm
Bally & Reipurth (06 “Birth of Stars & Planets” CUP = BR06)



HH 46/47 Spitzer
(Noriega-Crespo 04; BR06)

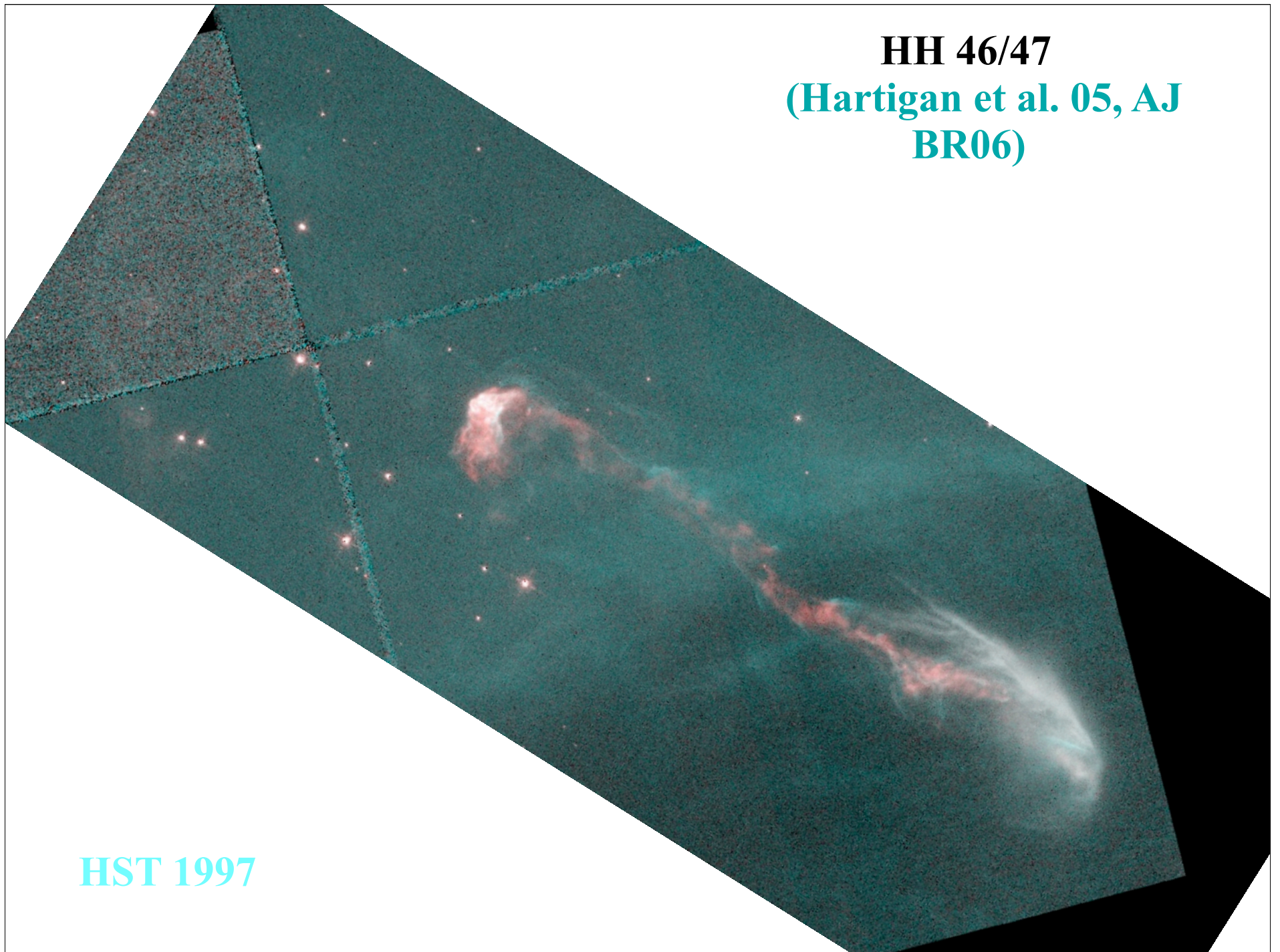
H₂ PAH 3.6, 4.5, 8 μm

HH 46/47
(Hartigan et al. 05, AJ
BR06)



HST 1994

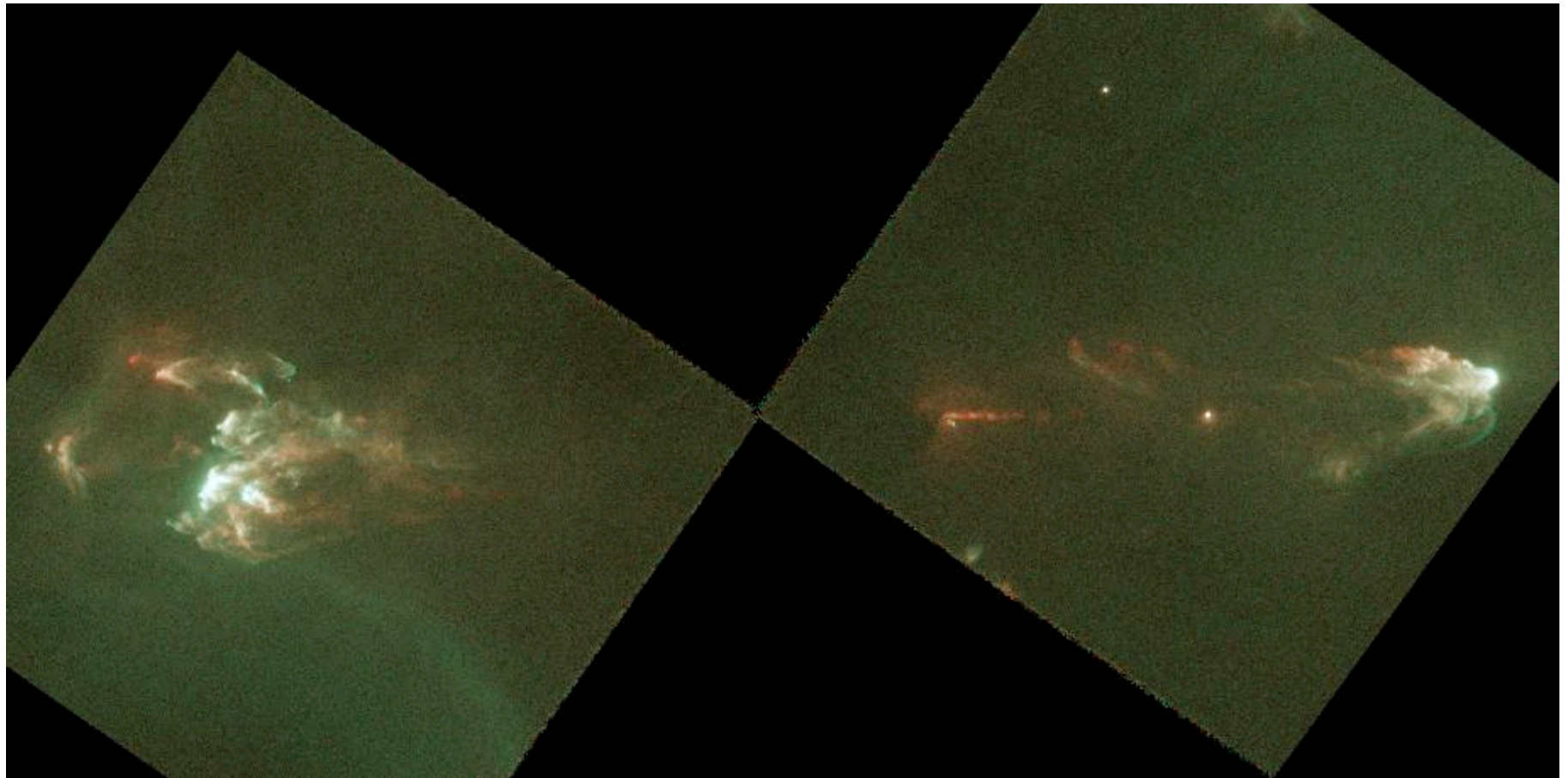
HH 46/47
(Hartigan et al. 05, AJ
BR06)



HST 1997

HH 2

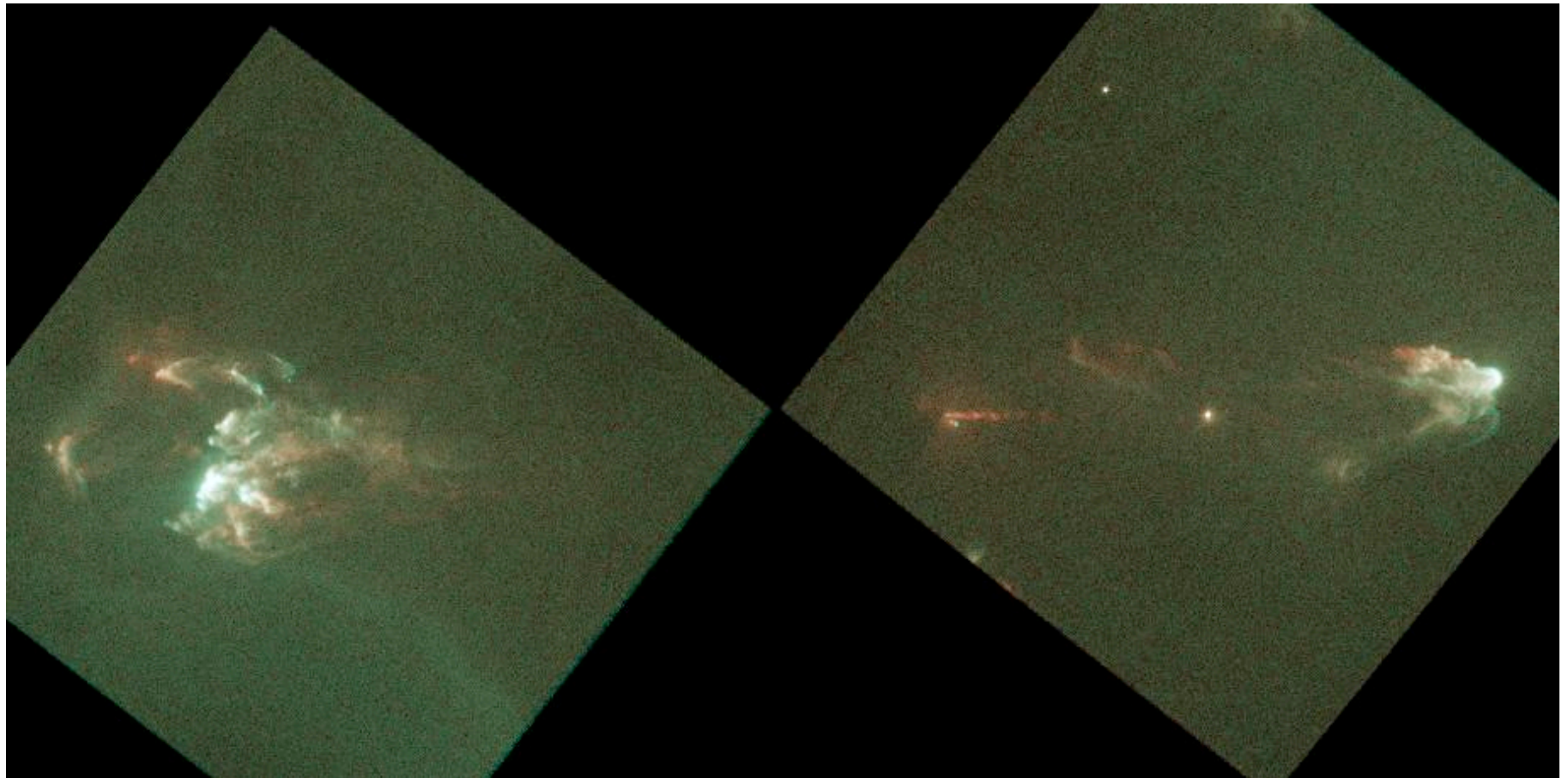
HH 1



HST 1997 - 1994

HH 2

HH 1



HST 1997 - 1994

HH 1 jet



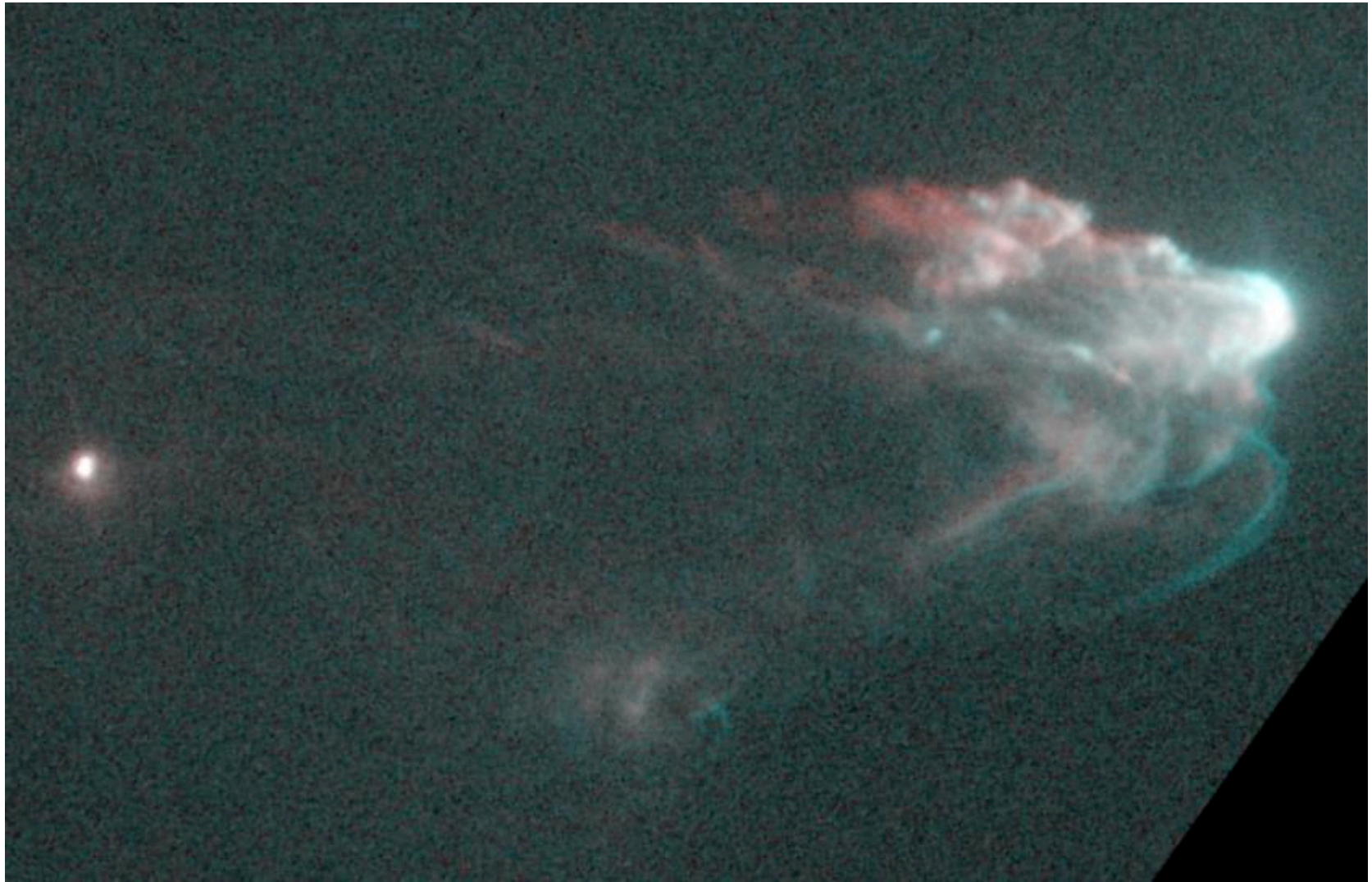
HST 1997 - 1994

HH 1 jet



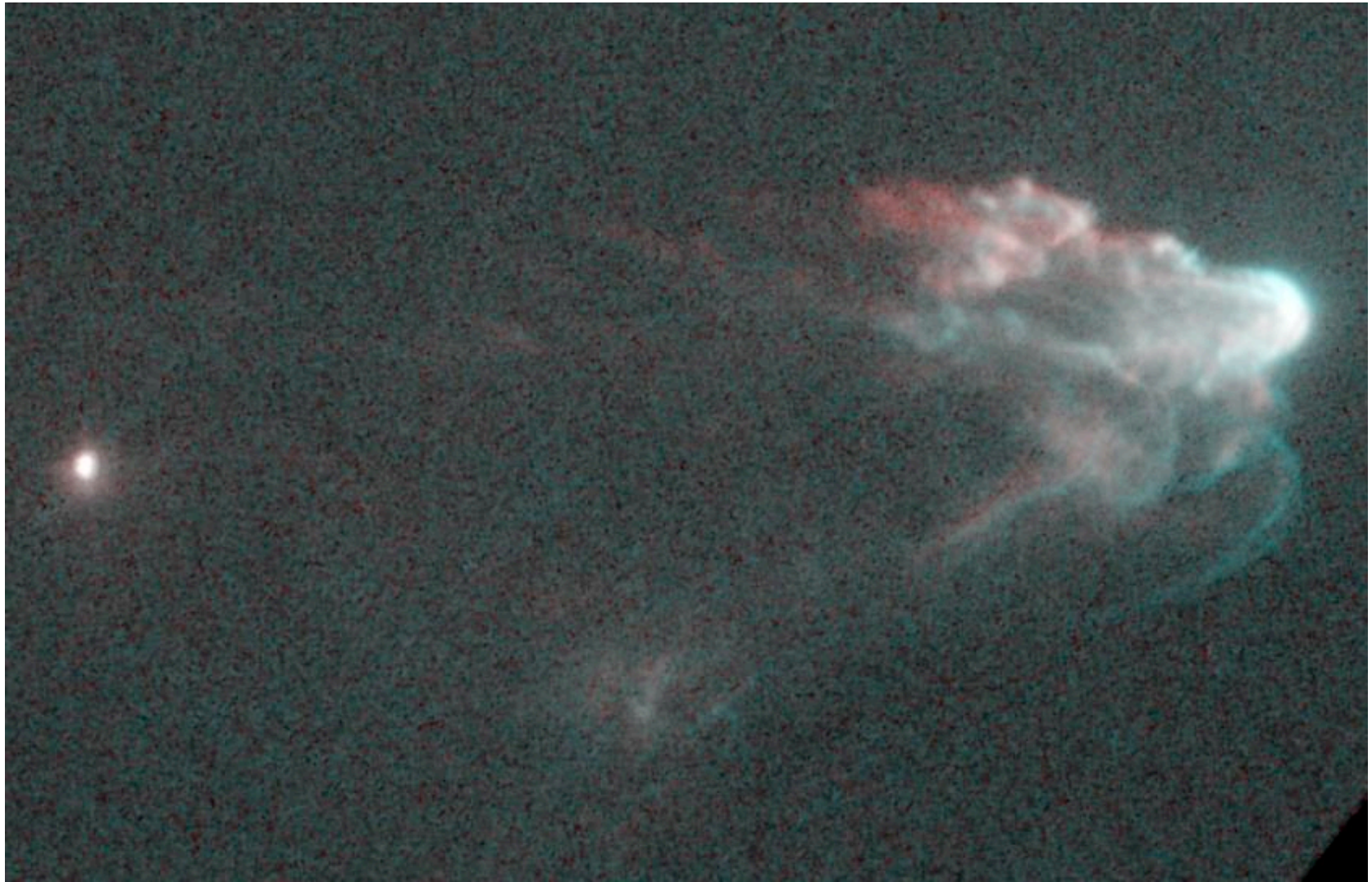
HST 1997 - 1994

HH 1



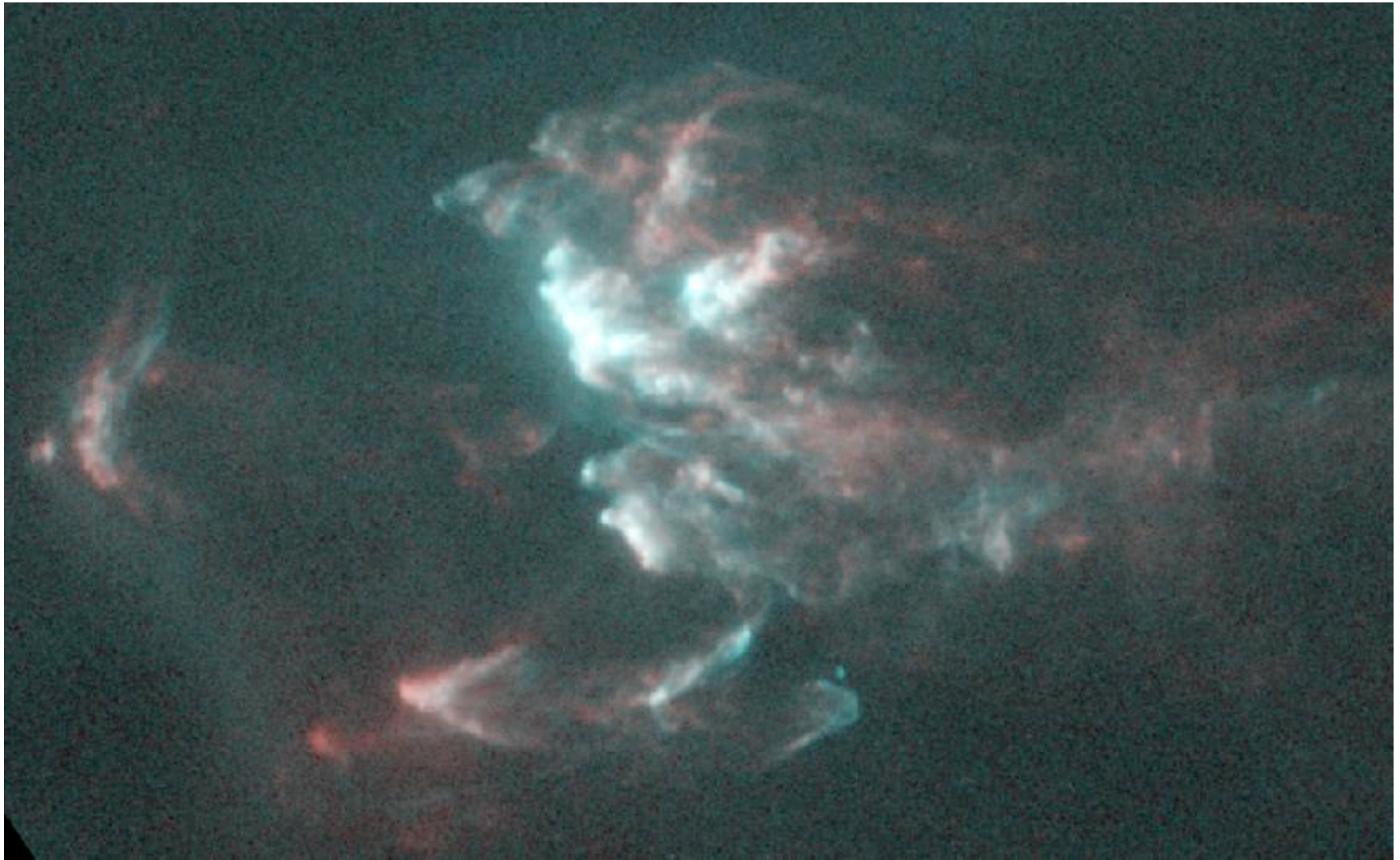
HST 1997 - 1994

HH 1



HST 1997 - 1994

HH 2



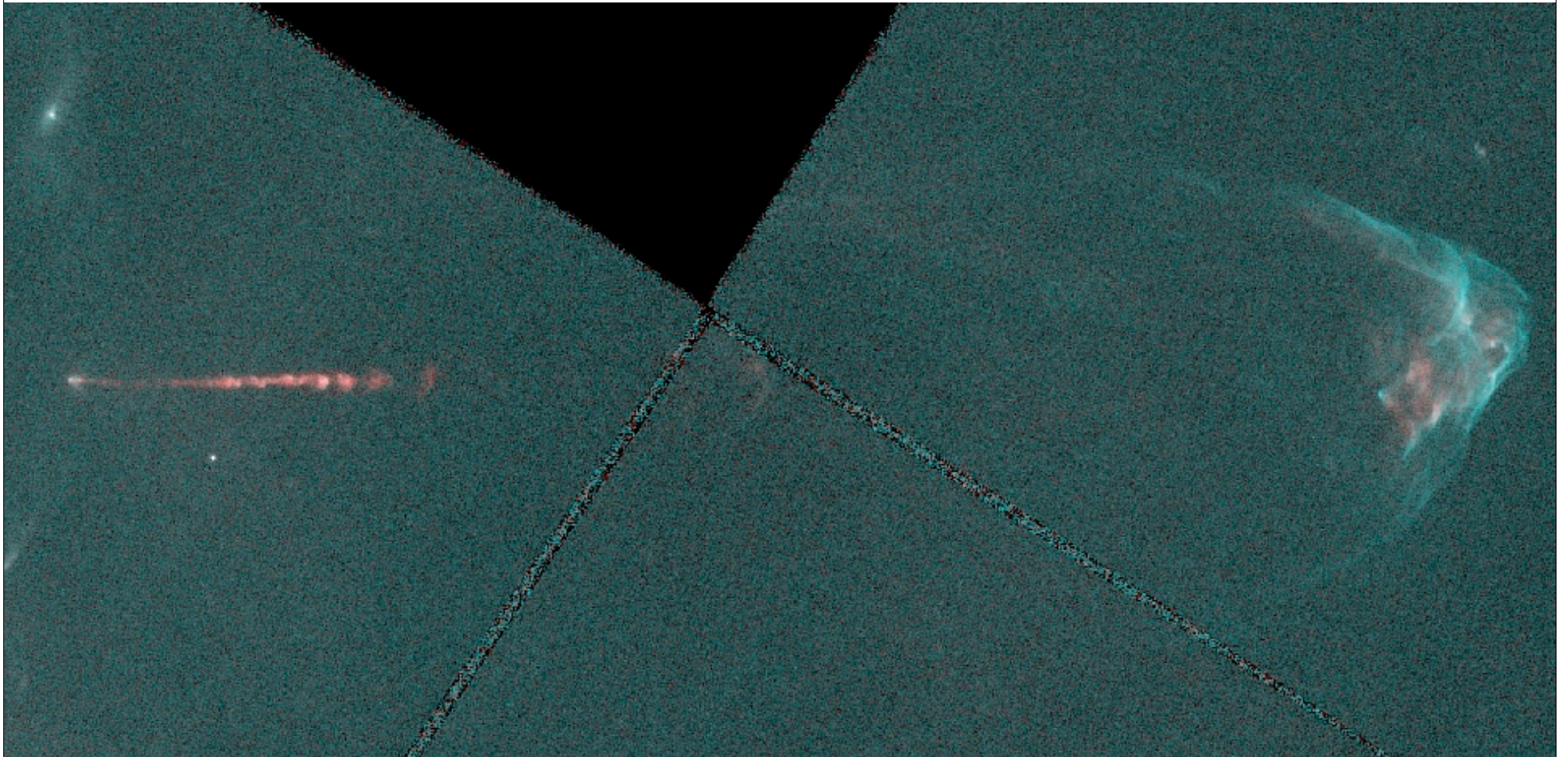
HST 1997 - 1994

HH 2



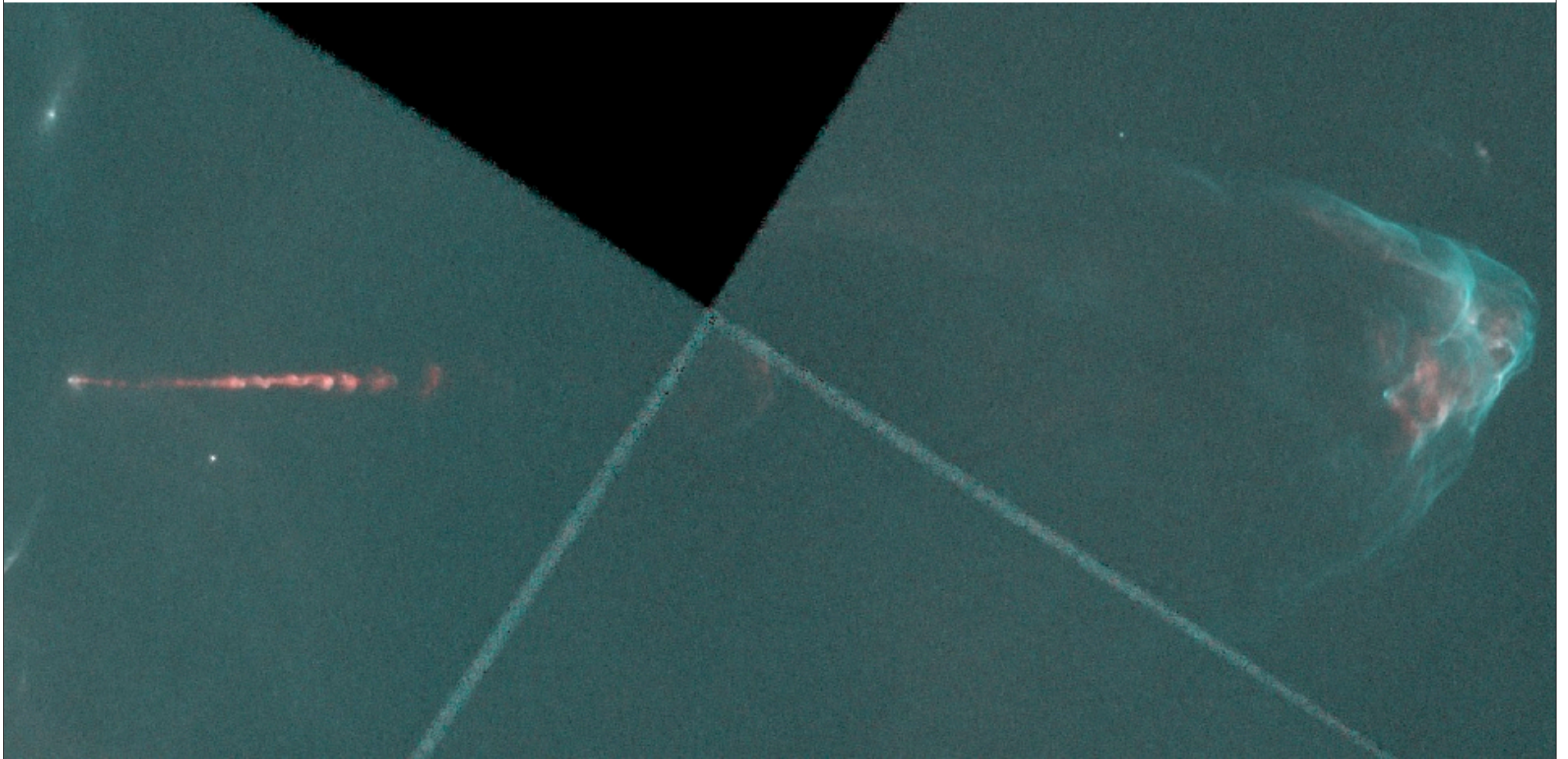
HST 1997 - 1994

HH 34



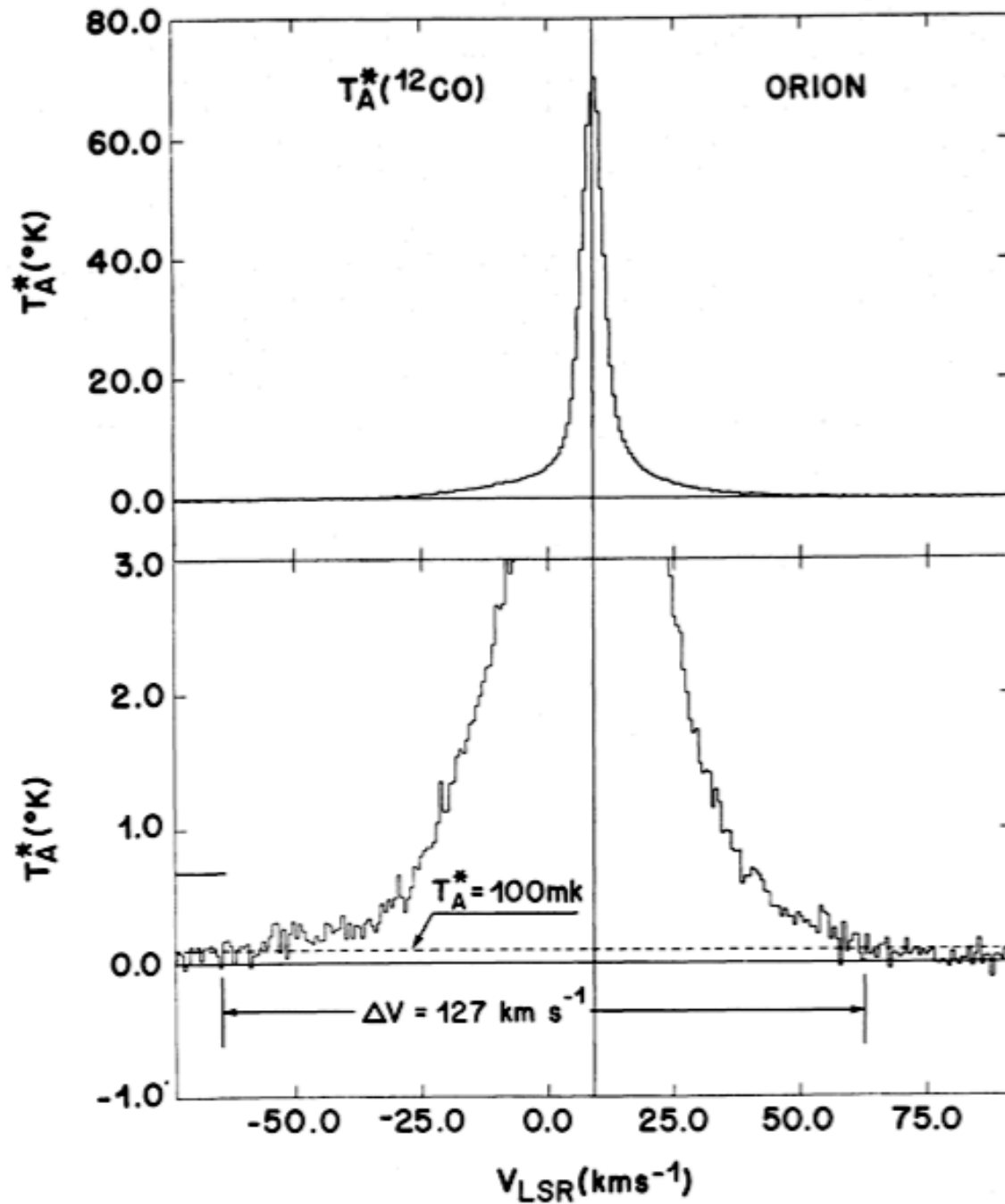
HST 1997 - 1994

HH 34



HST 1997 - 1994

Molecular Outflows



Molecular Outflows: Line Wings

Bally & Lada
1983

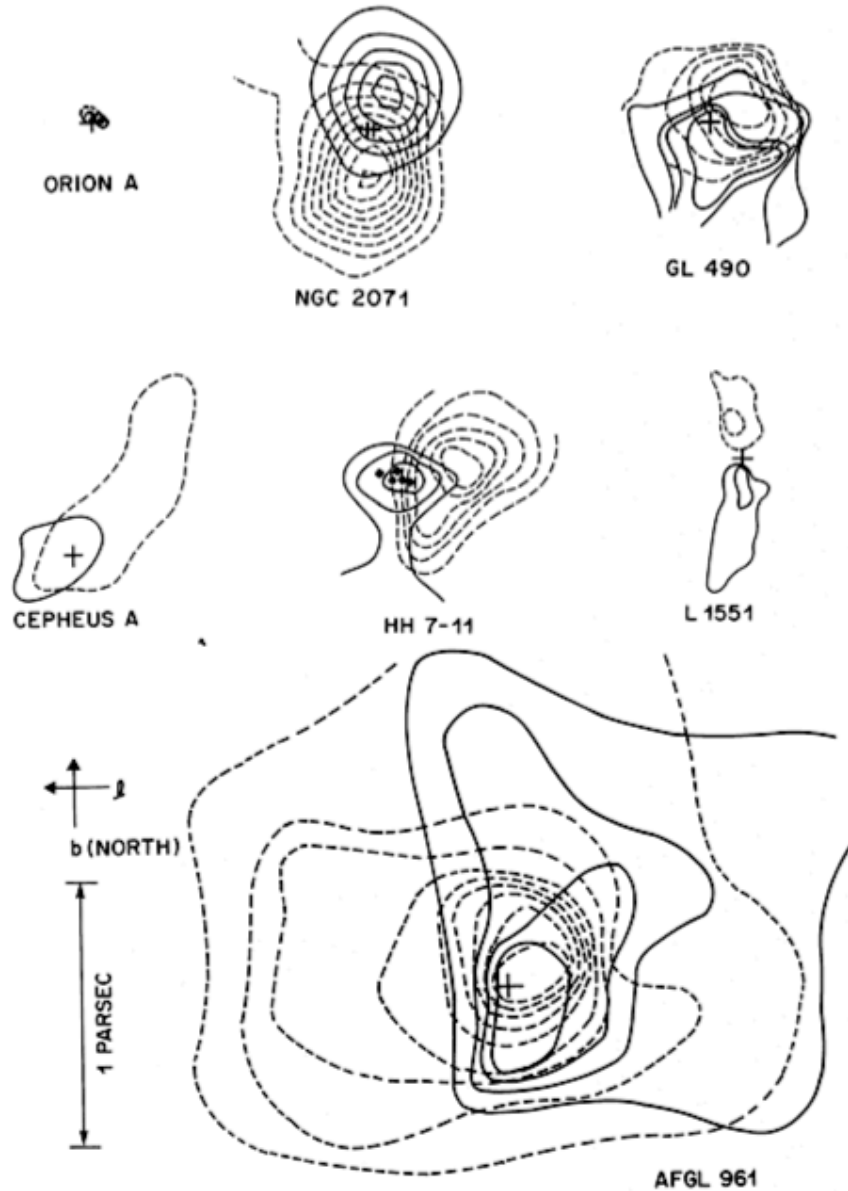


FIG. 13.—Maps of seven high-velocity molecular outflow sources in molecular cloud cores taken from the literature: NGC 2071 (Bally 1982*a*), L1551 (Snell, Loren, and Plambeck 1980), GL 490 (Lada and Harvey 1981), Cep A (Rodríguez, Ho, and Moran 1980), HH 7-11 (Snell and Edwards 1981), GL 961 (Lada and Gautier 1982), Orion A (Erickson *et al.* 1982). Solid lines are blueshifted wings, and dashed lines are the redshifted wings.

Molecular Outflows: Bipolarity Bally & Lada 1983

Molecular Outflows: Basic Properties

Bally & Lada 1983

838

BALLY AND LADA

Vol. 265

TABLE 4
PARAMETERS OF MAPPED MOLECULAR OUTFLOW SOURCES

Source	R_{\max}^a (pc)	R_{\min}^a (pc)	$(R_{\max} R_{\min})^{1/2}$ (pc)	R_{\max}/R_{\min}	M (M_{\odot})	Ref.	$\dot{M}V$ ($M_{\odot} \text{ yr}^{-1}$) km s $^{-1}$	$\frac{1}{2}MV^2$ (ergs)	L_{outflow} (L_{\odot})	$\langle n(\text{H}_2) \rangle$ (cm $^{-3}$)	$\frac{\int \text{Red Wing}}{\int \text{Blue Wing}}$
Orion	0.04	0.04	0.04	1.0	5	1	0.52	2.0×10^{47}	2600	3.8×10^5	...
AFGL 490	0.34	0.29	0.31	1.2	14	2.3	0.04	1.5×10^{47}	115	2.3×10^3	0.70
AFGL 961	1.18	0.97	1.07	1.2	20	3.4	0.007	8.0×10^{46}	11	0.8×10^2	3.72
NGC 2071	0.49	0.28	0.37	1.8	20	3.5	0.06	2.8×10^{47}	175	1.9×10^3	2.40
Cep A	0.50	0.08	0.20	6.2	10	6	0.012	6.2×10^{46}	25	6.0×10^3	2.90
S140	0.46	0.46	0.46	1.0	64	3	0.06	2.6×10^{47}	90.0	3.2×10^3	0.91
L1551	0.42	0.08	0.18	5.2	0.3	7	0.0002	6.7×10^{43}	0.2	2.5×10^2	0.56
HH 7-11	0.40	0.21	0.29	1.9	4.0	8	0.004	1.6×10^{46}	6.5	7.9×10^2	4.26
HH 24-26	0.25	0.19	0.22	1.3	6.3	8	0.006	1.4×10^{46}	6.9	2.9×10^3	2.0
Mon R2	2.09	0.70	1.21	4.0	100	9,10	0.02	2.3×10^{47}	24.0	2.8×10^2	1.18
Serpens	1.11	0.65	0.85	1.7	...	10	0.9
T Tauri	0.15	0.15	0.15	1.0	0.1	11	0.00003	4.2×10^{43}	0.01	1.4×10^2	...

^aSource sizes corrected for beam size.

REFERENCES.—(1) Solomon, Huguenin, and Scoville 1981. (2) Lada and Harvey 1981. (3) Lada 1982. (4) Lada and Gautier 1982. (5) Bally 1982*a*. (6) Rodriguez, Ho, and Moran 1980. (7) Snell, Loren, and Plambeck 1980. (8) Snell and Edwards 1981. (9) Loren 1981. (10) This paper. (11) Edwards and Snell 1981.

Molecular Outflows: Mechanical Luminosity and Momentum Flux

Bally & Lada 1983

No. 2, 1983

HIGH-VELOCITY MOLECULAR FLOWS

841

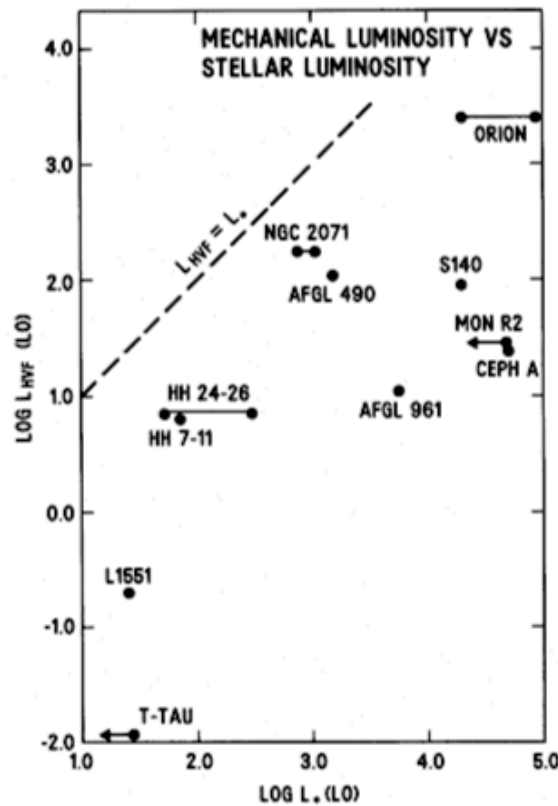


FIG. 16.—Plot of the flow mechanical luminosity vs. total bolometric luminosity of the associated infrared sources. Also shown is the relation $L_{HVF} = L_{*}$.

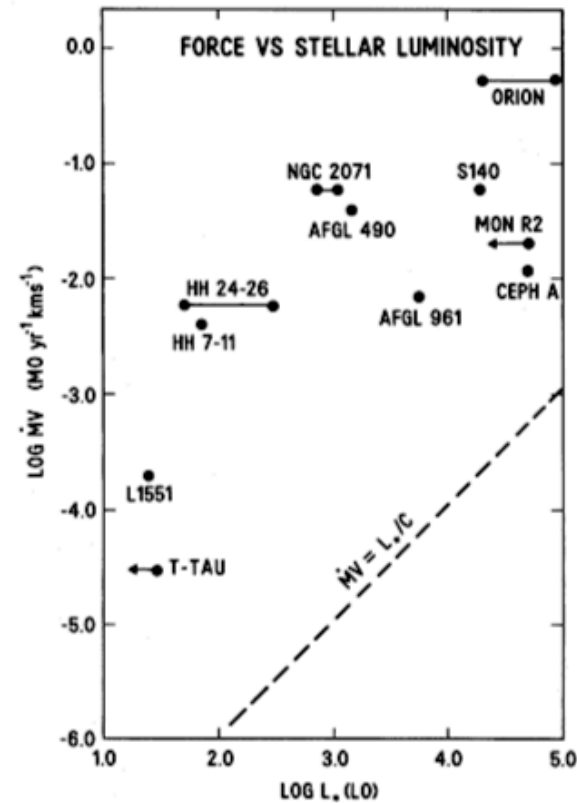
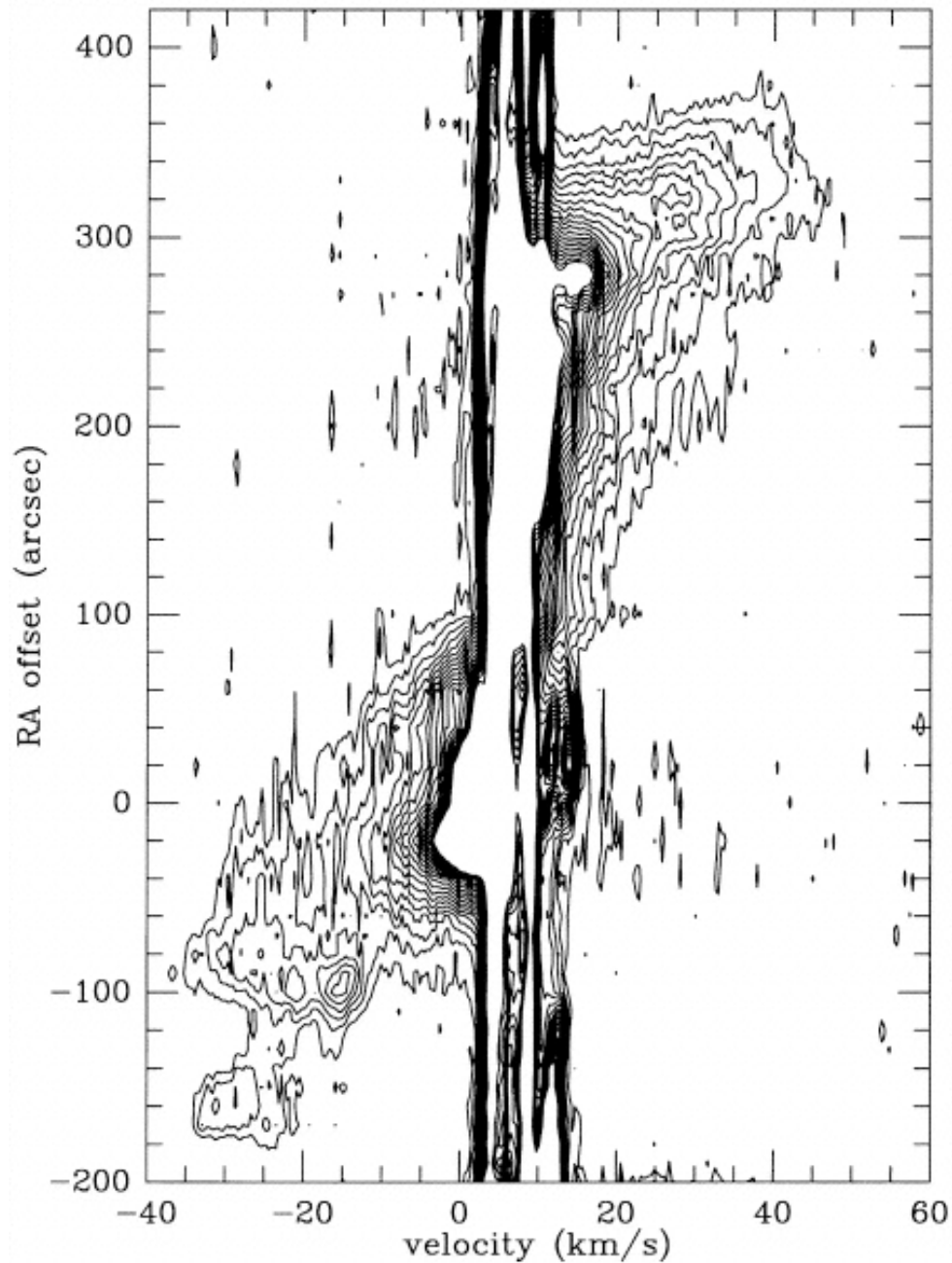


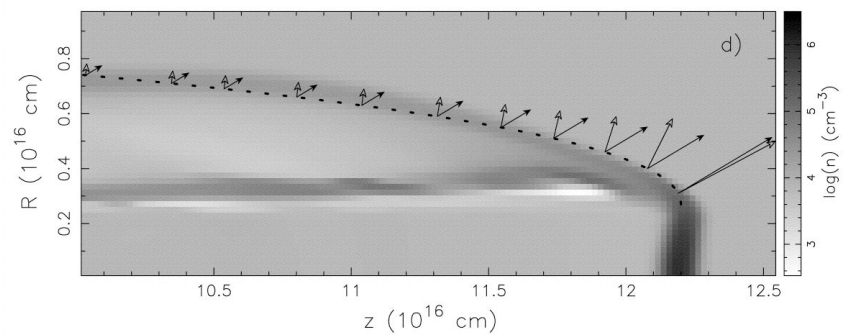
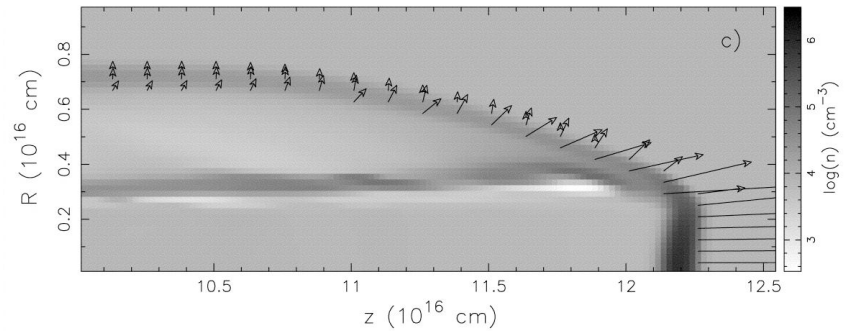
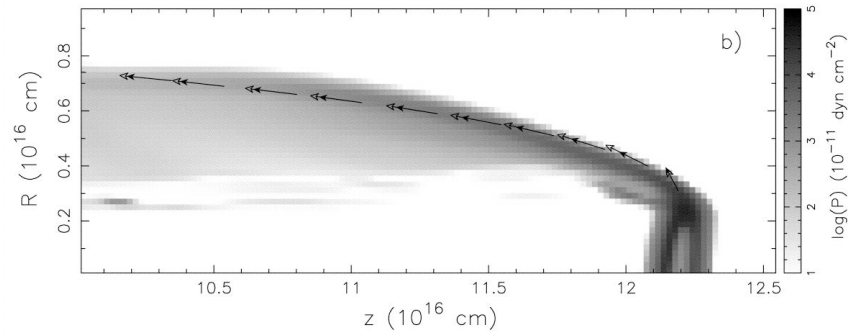
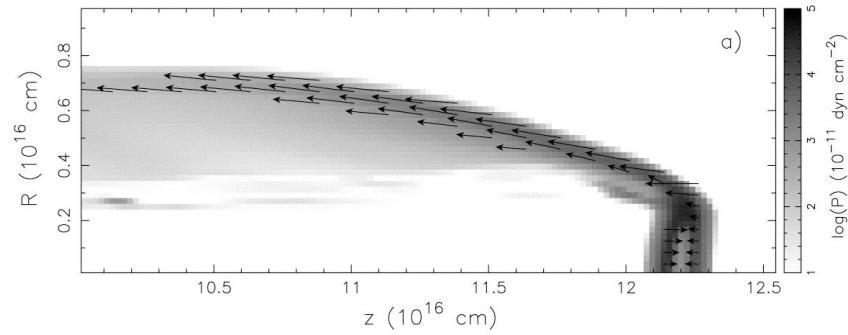
FIG. 17.—Plot of MV for the flows vs. total bolometric luminosity of the associated infrared sources. Also shown is the relation $MV = L_{*}/C$.



Molecular
Outflow: the
“Hubble Law”
NGC 2264 G
Fich & Lada
1998

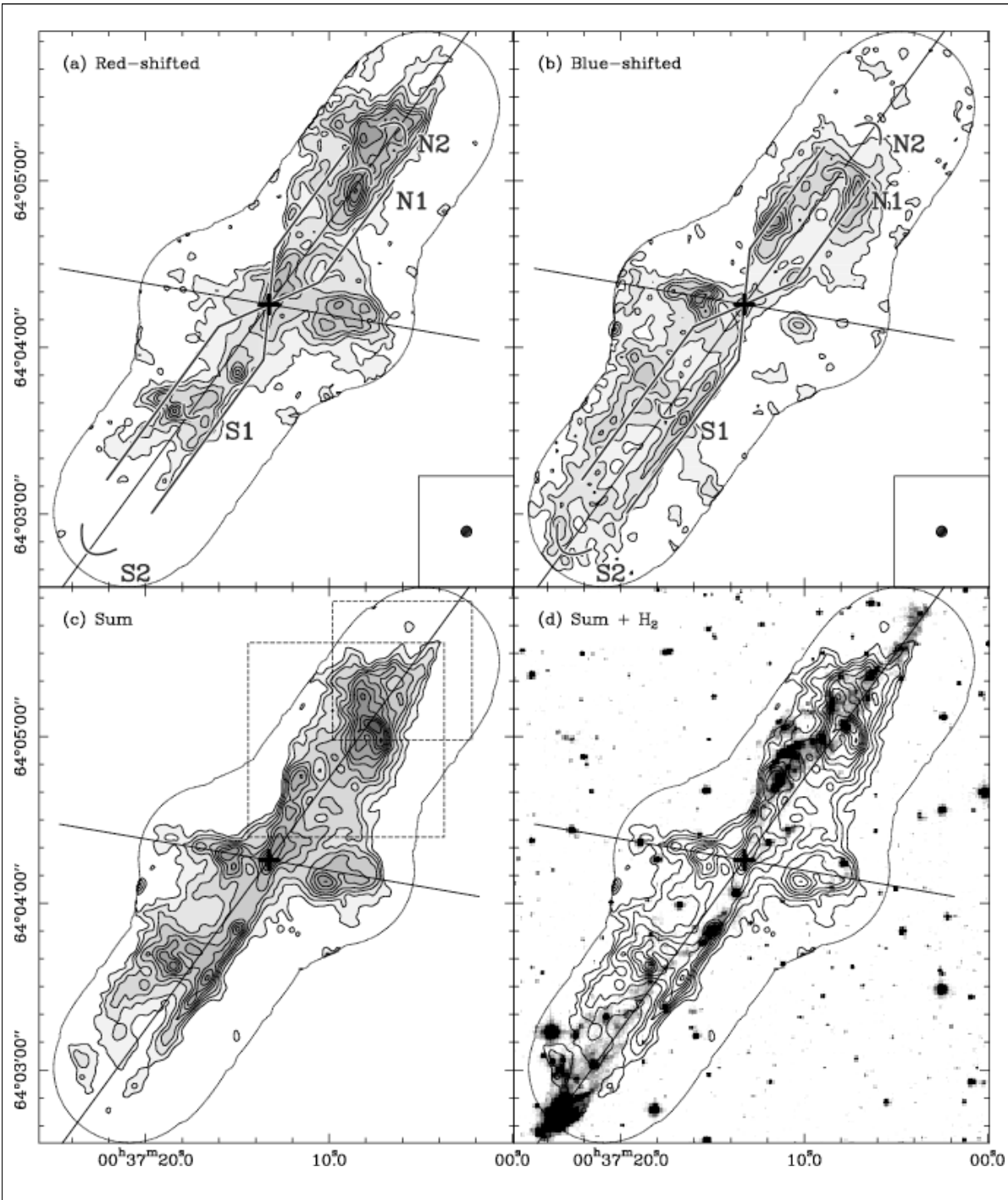
Distinguishing between Wind and Jet Models Lee et al. 2001

Bow shock



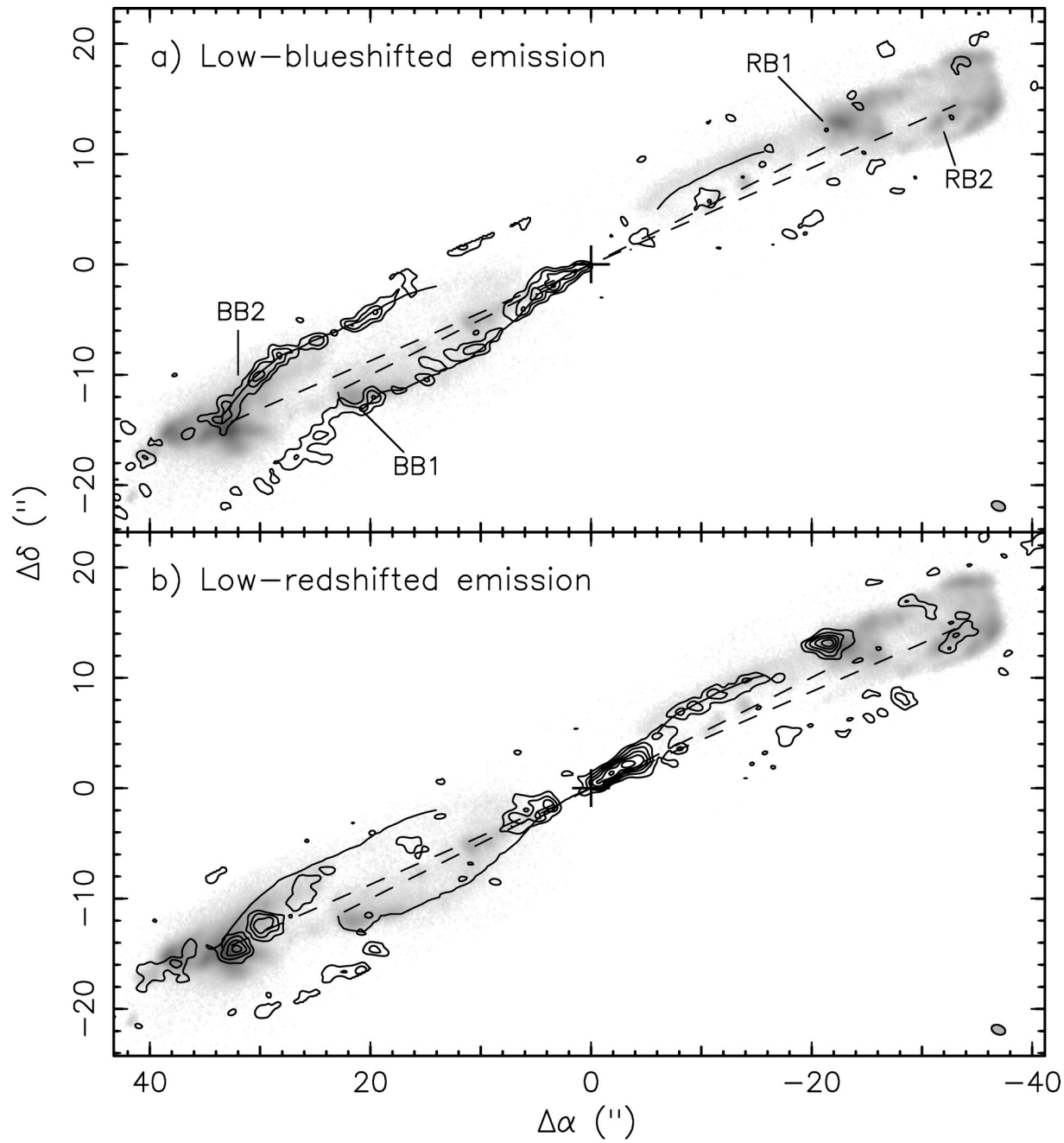
Wind

HH 288:
Contours: CO
(2-1)
Greyscale: H₂

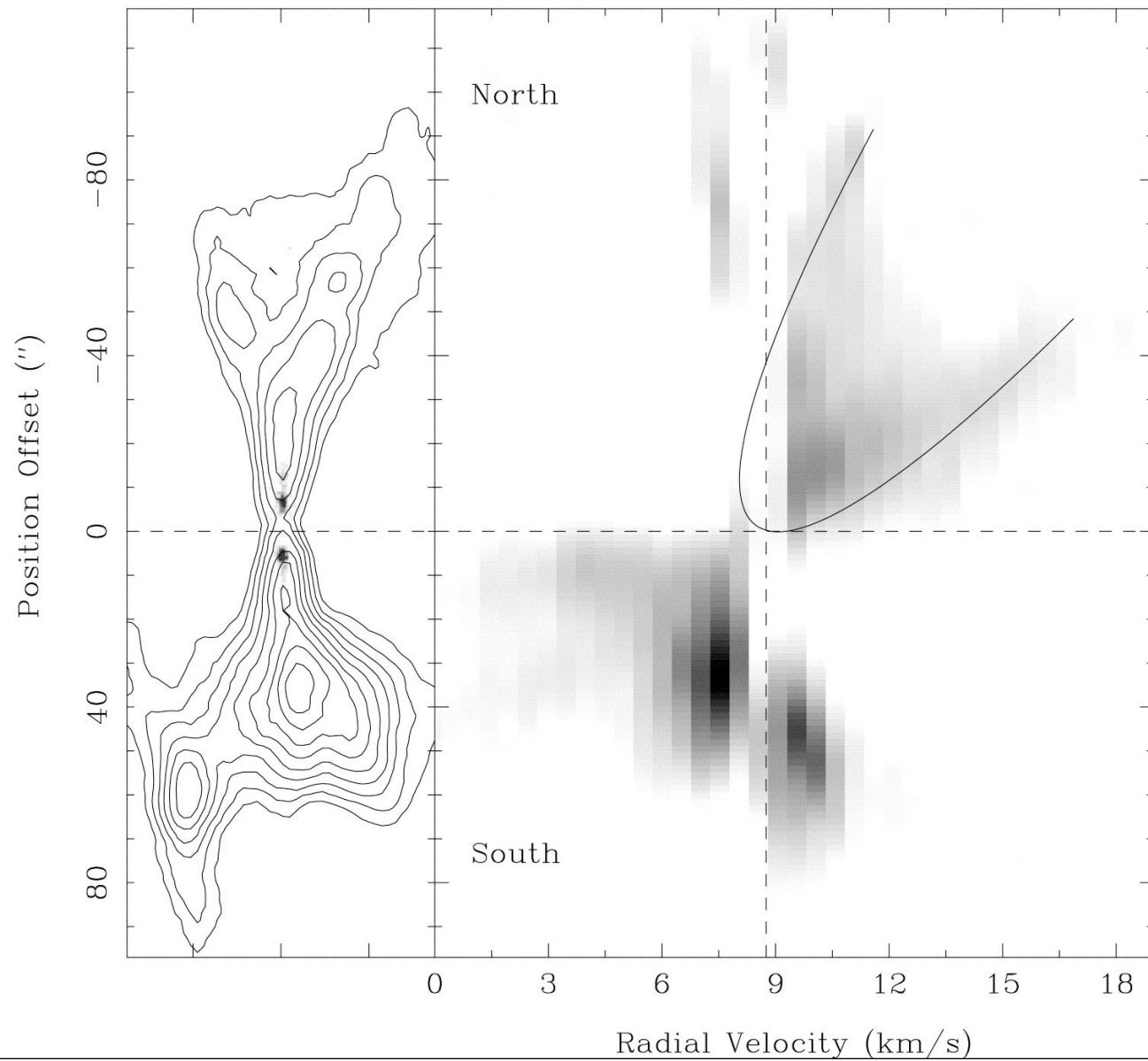


HH 211

Contours: CO
(2-1)

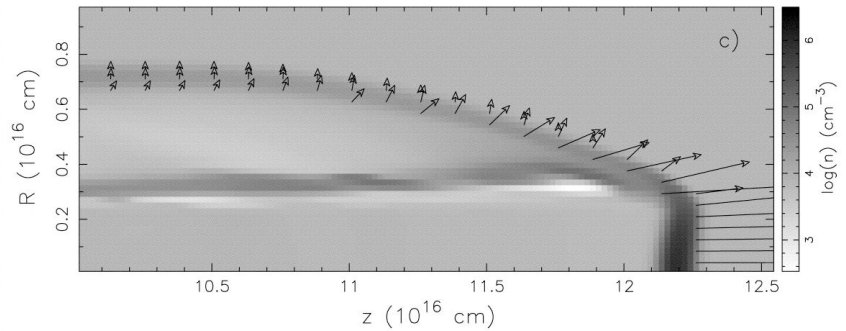
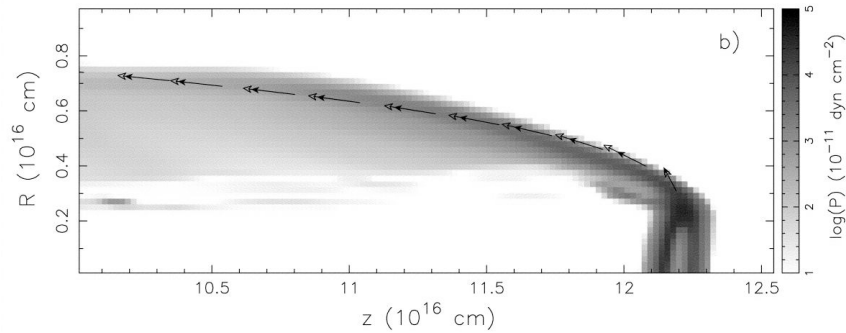
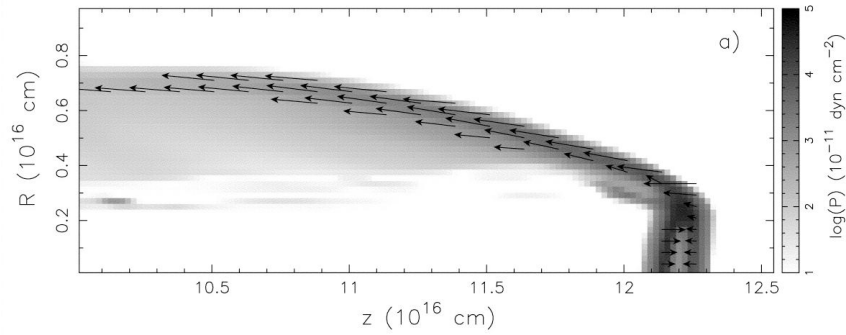


VLA 05487: example of wind (Lee et al. 2001)

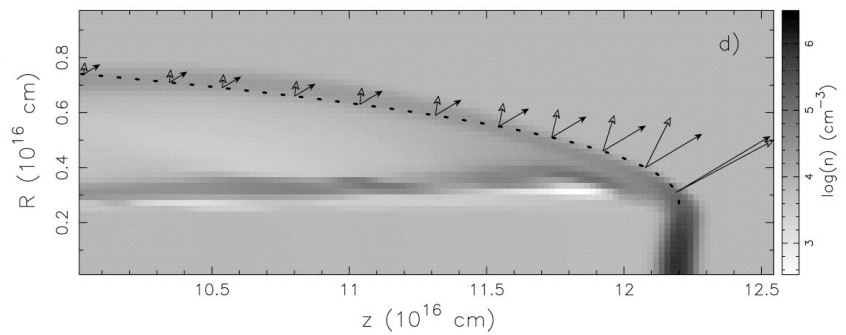


Distinguishing between Wind and Jet Models Lee et al. 2001

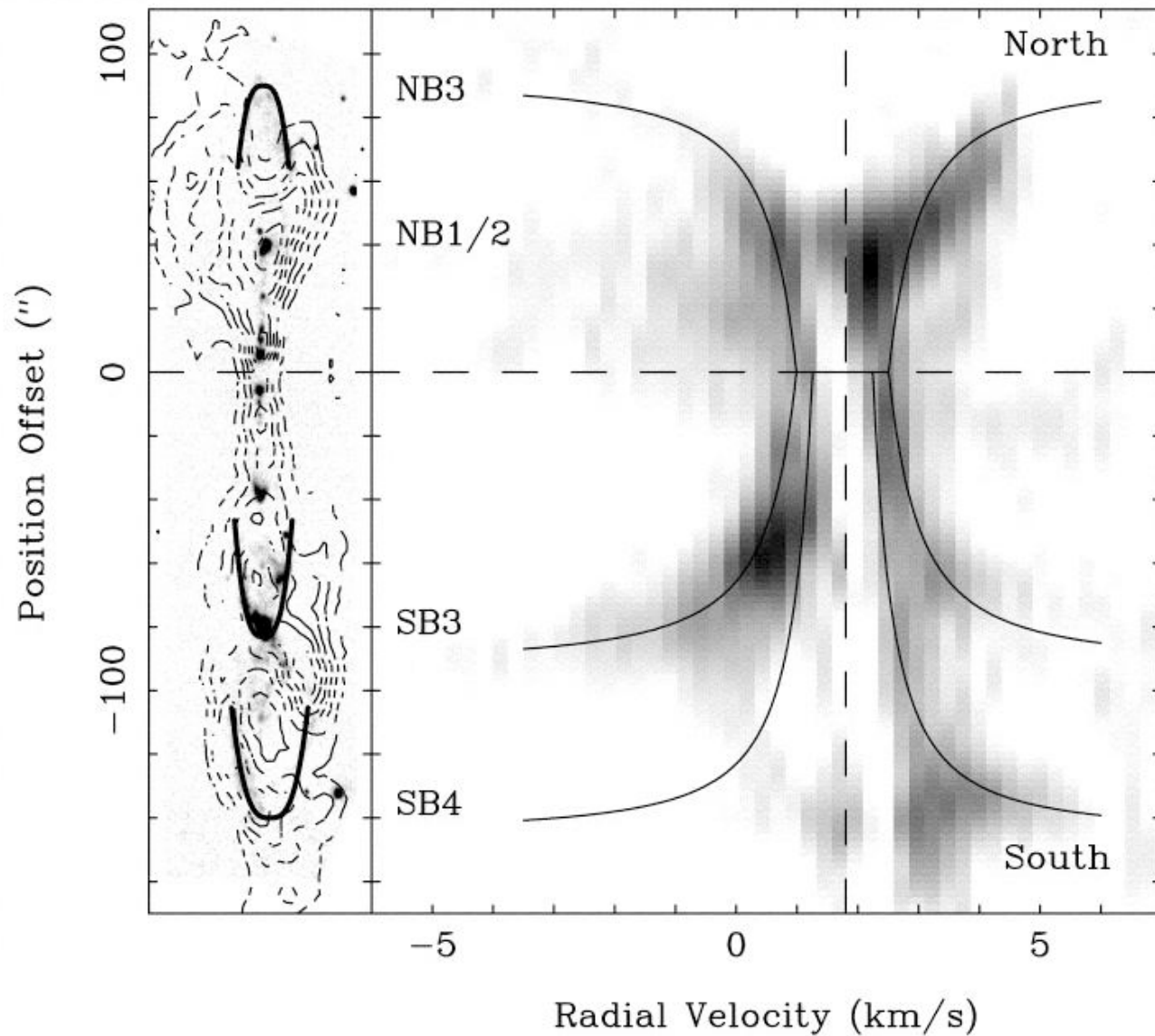
Bow shock



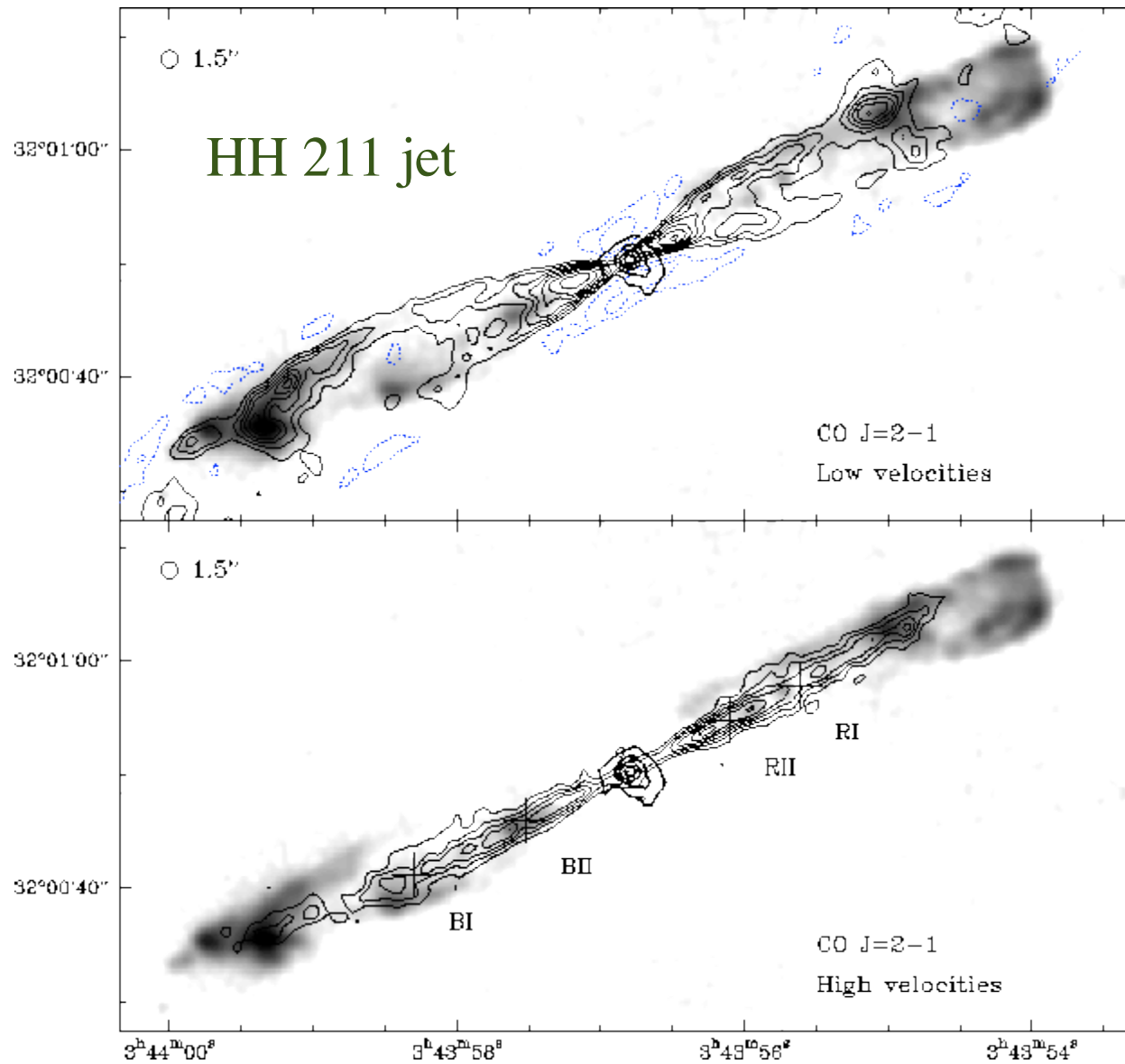
Wind



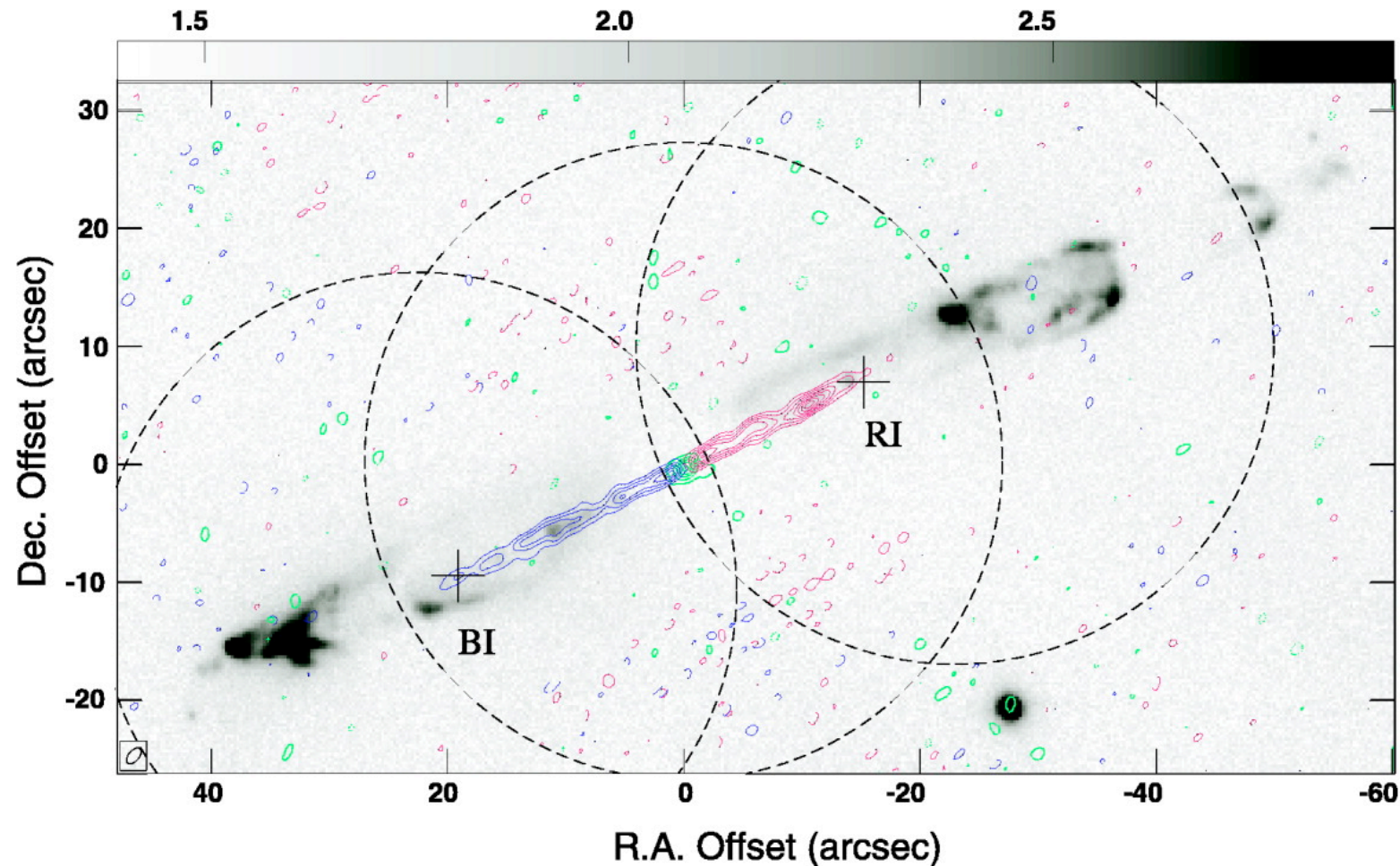
HH 212: example of jet (Lee et al. 2001)



Detecting *Jets* in Molecular Gas

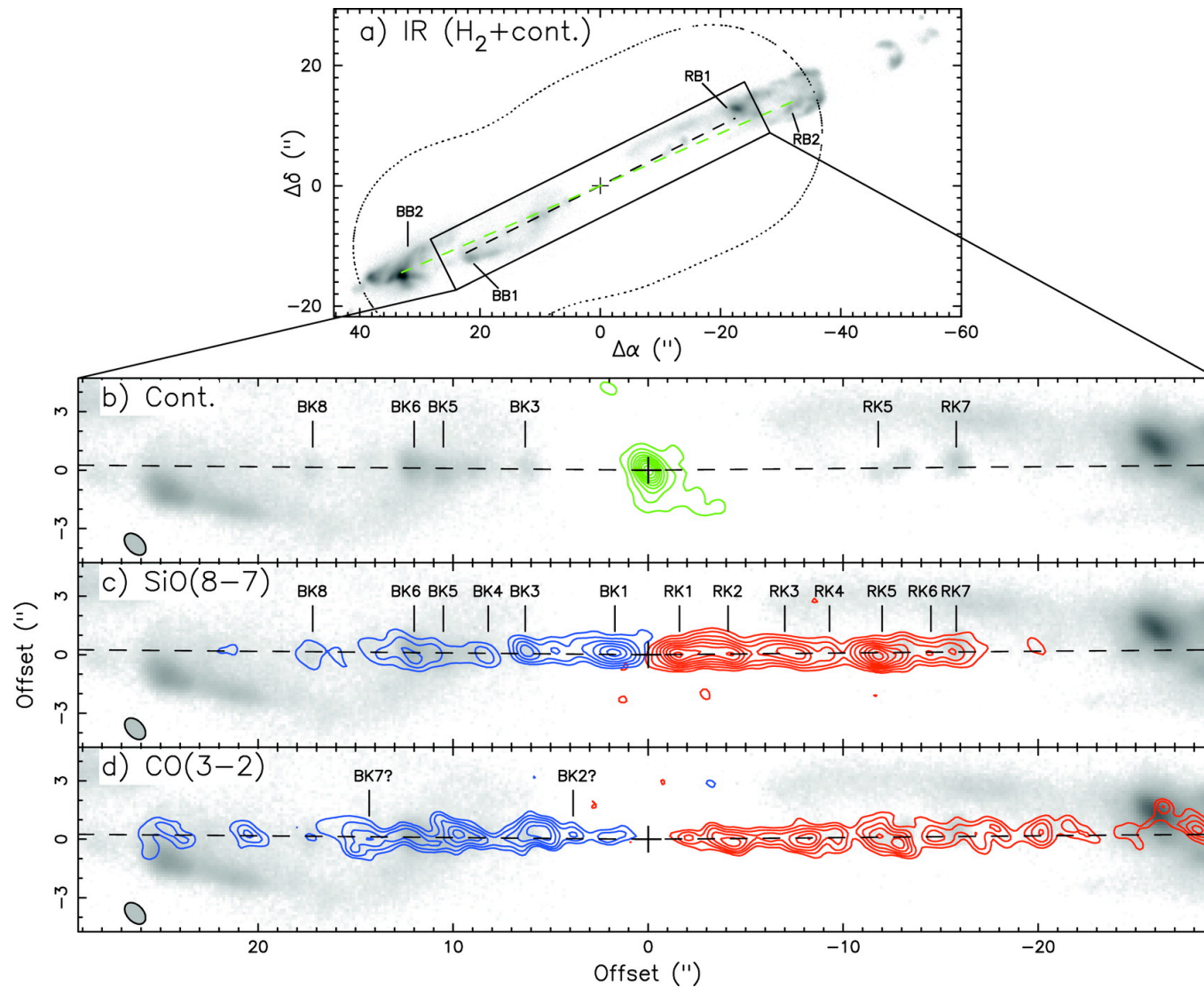


Detecting *Jets* in Molecular Gas

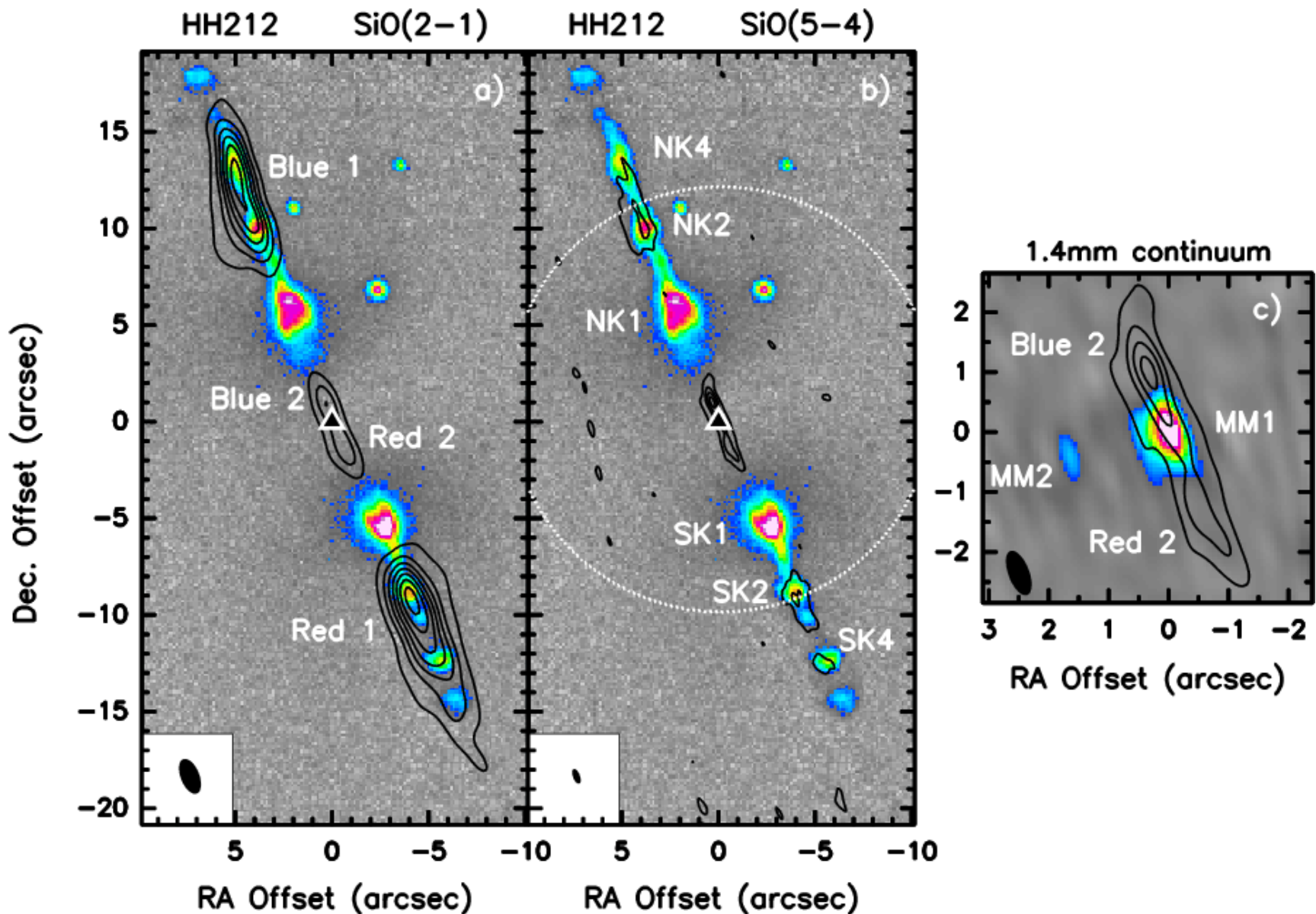


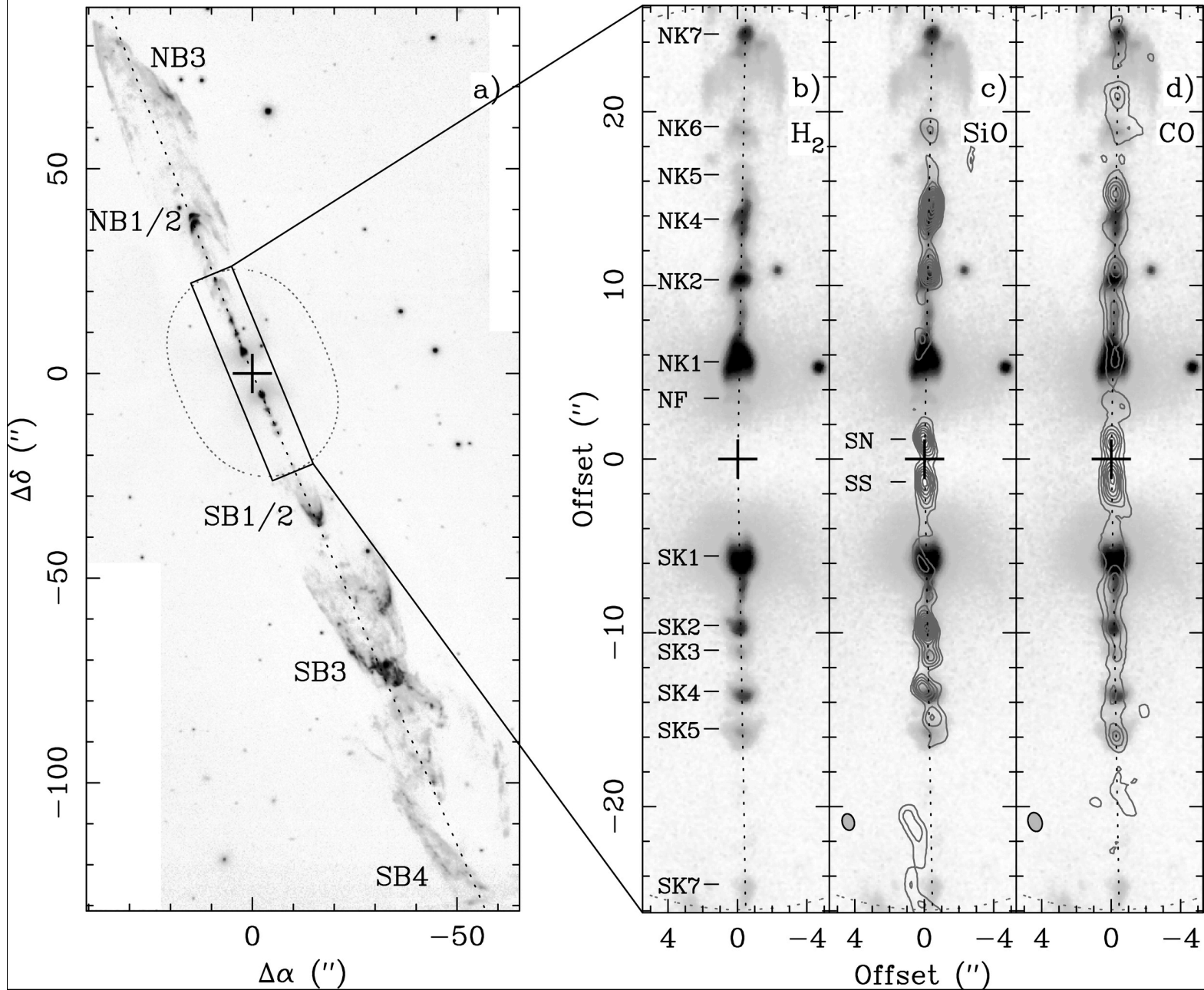
SiO mm-wave rotational lines are an excellent tracer of jets:
abundance enhanced by a few orders of magnitude in jets

HH 211 Lee et al. 2007



SiO HH 212 Codella et al. 2008





HH
212
Lee et
al.
2007

HH 212 Lee et al. 2007

